THE JOURNAL OF PHYSICAL CHEMISTRY B

Article

pubs.acs.org/JPCB

Molecular Aggregation in Binary Mixtures of Pyrrolidine, *N*-Methylpyrrolidine, Piperidine, and *N*-Methylpiperidine with Water: Thermodynamic, SANS, and Theoretical Studies

Wojciech Marczak,[*,†,‡] Mikhail A. Varfolomeev,[‡] Ilnaz T. Rakipov,[‡] Piotr Lodowski,[§] Katarzyna Kowalska-Szojda,[§] Marta Łężniak,[∥] László Almásy,[⊥,#] and Adél Len[⊥,○]

[†]Institute of Occupational Medicine and Environmental Health, Kościelna 13, 41-200 Sosnowiec, Poland

[‡]Department of Physical Chemistry, Kazan Federal University, Kremlevskaya Str. 18, 420008 Kazan, Russian Federation

[§]Institute of Chemistry, University of Silesia, Szkolna 9, 40-006 Katowice, Poland

[∥]Institute of Materials Science, University of Silesia, 75 Pułku Piechoty 1A, 41-500 Chorzów, Poland

[⊥]Wigner Research Centre for Physics, POB 49, Budapest 1525, Hungary

[#]State Key Laboratory Cultivation Base for Nonmetal Composites and Functional Materials, South-West University of Science and Technology, Mianyang, China

[○]Faculty of Engineering and Information Technology, University of Pécs, Boszorkány út 2, 7624 Pécs, Hungary

Supporting Information

ABSTRACT: Piperidine and *N*-methylpiperidine hydrates aggregate in liquid aqueous solutions due to hydrogen bonds between hydration water molecules. No such effects occur in the mixtures of the amines with methanol, that supports the idea of active role of water solvent in the aggregation. However, the question of contributions in thermodynamic functions due to specific interactions, van der Waals forces, and the size and shape of the molecules remains open. In the present study, limiting partial molar enthalpies of solution of pyrrolidine, *N*-methylpyrrolidine, piperidine, and *N*-methylpiperidine in water and methanol and *vice versa* were measured and compared with those assessed from theoretically calculated molecular interaction energies using a simple "chemical reaction" model. Nearly quantitative agreement of the enthalpies was achieved for the systems studied, except the amines in water. The latter required an empirical hydrophobic hydration term to be considered. The hydrogen bonds formation and breaking which accompany the mixtures formation leads to considerable excess volumes, while the size of the solute molecules is manifested rather in the compressibility of aqueous solutions. SANS evidenced that aqueous solutions are microheterogeneous on the nanometer-order length scale. The propensity to promote phase separation increases in the order: *N*-methylpiperidine < *N*-methylpyrrolidine < piperidine < pyrrolidine.

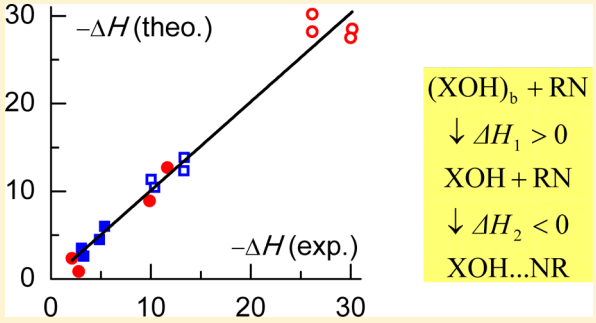

1. INTRODUCTION

Previous studies of liquid binary mixtures of piperidine and *N*-methylpiperidine with water revealed heterogeneities in the nanometer-length scale, probably caused by aggregation of the amine-water cross-associates due to O−H···O bonds between the hydration water molecules. Small-angle neutron scattering (SANS) experiments point to concentration fluctuations in the *N*-methylpiperidine system and to a microphase separation with two characteristic lengths in that of piperidine. Differences between the two systems were manifested also in the thermodynamic excesses of molar volume, molar isentropic compression and molar isobaric expansion, while theoretically calculated stabilization energies of water−amine complexes differed rather slightly.[1,2] Observed regularities tempted us to complete the study with binary aqueous solutions of another pair of cyclic amines, namely pyrrolidine and *N*-methylpyrrolidine, and to compare the results.

To the best of our knowledge, the only comparison available in the literature is that based on the heats of solution in water.[3] The smaller negative heats of solution of secondary amines (pyridine and pyrrolidine) in water, in comparison with those of the tertiary ones (respective *N*-methyl-substituted compounds), was explained qualitatively as a consequence of breaking the N−H···N bonds in the former. Differences in the entropy of hydration were attributed to the formation of water clusters around the solute molecule. Studies of pyrrolidine-water system concerned densities,[4,5] viscosities[5] and speeds of

Received: October 11, 2016
Revised: March 19, 2017
Published: March 21, 2017

DOI: 10.1021/acs.jpcb.6b10262
J. Phys. Chem. B 2017, 121, 3070−3086

ultrasound[6] in binary and ternary[7] mixtures piperidine + pyrrolidine + water. An addition of pyrrolidine or piperidine to water rapidly decreases the surface tension, and the values of surface entropy for the two systems are equal one to another and independent of the mixtures composition.[8] Vapor−liquid equilibrium curves for pyrrolidine-water system show positive deviation from Raoult's law, but the mixture remains zeotropic, while pyrrolidine with ethanol forms negative azeotrope.[9] The corrected preferential solvation parameters point to self-preference of the pyrrolidine and water molecules in binary mixture due to their interactions rather than differences in their volumes.[10] Single relaxational absorption determined in the ultrasound attenuation studies of aqueous solutions of pyrrolidine in the frequency range 3.0−220 MHz was explained by a proton transfer reaction, while aqueous piperidine showed also another relaxation process in this frequency range, associated with an aggregation of nonionized molecules.[11]

Important difference between piperidine and *N*-methylpiperidine (as well as between pyrrolidine and *N*-methylpyrrolidine) is the ability to self-association of the former due to N−H···N bonds. In crystals, neat piperidine and pyrrolidine form chains of hydrogen-bonded molecules.[12−14] However, the contribution of van der Waals interactions in the sublimation enthalpy surpasses that of hydrogen bonding at least for piperidine.[14] The pyrrolidine ring is by one methylene group smaller than that of piperidine, while *N*-methylpyrrolidine is its structural isomer incapable of N−H···N bonding. Thus, undertaking the present study we hoped to gather information that would help to tell apart the contributions due to hydrogen bonds, van der Waals molecular interactions, and those related to the size and shape of the molecules (Figure 1).

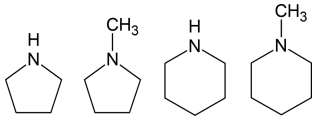

Figure 1. Molecules of pyrrolidine, *N*-methylpyrrolidine, piperidine, and *N*-methylpiperidine.

Another reason for interest in these systems is that piperidine and *N*-methylpiperidine act as clathrate promoters in water. Clathrate hydrates are promising materials in practical applications because of their high gas storage capacity.[15−18] Moreover, information about crystal structures helps to suggest reliable models of molecular order in liquids, which otherwise must be rather speculative at the present state of knowledge. Obviously, clathrate-like structures in the liquid state are dynamic, contrary to solid clathrate hydrates which are stable in time, although even the latter may undergo deformations due to changes of temperature and pressure.[19]

In the solid state, pyrrolidine and piperidine with methane forms sII clathrate hydrates in aqueous solutions at elevated pressures,[20] while sH clathrates of *N*-methylpiperidine arise in similar conditions.[15] Recently, crystal structures of pyrrolidine hemi- and hexahydrates were reported.[21] In the former, two amine molecules are hydrogen-bonded with one water molecule. The solid hexahydrate is a semiclathrate structure with guest amine molecules participating in the hydrogen-bonded network of the host water. It seems reasonable to presume that *N*-methylpyrrolidine also forms solid hydrate clathrates or semiclathrates, although no information about such structures is available in the literature. The structures of the solid systems support the supposition about the role of water as an active solvent causing molecular aggregation in liquid aqueous solutions of cyclic aliphatic and aromatic amines, suggested to explain e.g. phase splitting of binary mixtures of *N*-methylpiperidine and 2,6-dimethylpyridine with water at temperatures slightly above the room one, and relaxation times of the nanoseconds order of magnitude in these mixtures, determined in the ultrasound absorption experiments.[1,22,23]

In the present work, we report limiting partial molar enthalpies of solution of pyrrolidine, *N*-methylpyrrolidine, piperidine and *N*-methylpiperidine in water and methanol, and *vice versa*, as well as enthalpy effects of hydrogen bonding assessed according to Solomonov's method.[24−30] The experimental enthalpies were compared with those estimated from theoretically calculated energies of binary molecular interactions. Molecular order in mixtures of finite concentration was suggested on the basis of the SANS results and applied in the discussion of isentropic compressibilities and thermodynamic excesses of molar volume and molar isobaric thermal expansion.

2. THEORETICAL CALCULATIONS

The following systems were studied by quantum chemical methods: 1:1 hydrogen-bonded complexes of pyrrolidine and *N*-methylpyrrolidine with water and methanol, 1:1 and 1:2 complexes of piperidine with methanol, as well as pyrrolidine and *N*-methylpyrrolidine dimers. Association energy of complexes and dimers was defined as supermolecule interaction energy, $\Delta E[A{\cdot}nB]$, which was calculated as the difference between the sum of the energies of the interacting monomers, E_A and E_B, and the energy of the complex, $E_{A{\cdot}nB}$:

$$\Delta E[A{\cdot}nB] = (E_A + nE_B) - E_{A{\cdot}nB} \quad (1)$$

where the symbols A and B stand for the interacting molecules, different for complexes and the same for dimers, and $n = 1$ and $n = 2$ for the 1:1 and 1:2 complexes, respectively. E_{AB}, E_A, and E_B, were evaluated at the same level of theory using the same basis set and the same quadrature in DFT calculations. Interaction energies were calculated from the density functional theory (DFT) with the B3LYP exchange-correlation functional, and from the second-order Møller−Plesset perturbation theory (MP2)[31] using the Dunning's augmented correlation consistent polarized valence double-ξ (aug-cc-pVDZ) basis set.[32−35] The isolated molecules geometries and those of the complexes were fully optimized at the DFT/B3LYP level of theory. These geometries were applied in the MP2 single point energy calculations. Additionally, geometries of the complexes of pyrrolidine and *N*-methylpyrrolidine were also fully optimized at the MP2 level of theory. Because association energies obtained from full geometry optimization at MP2 level and from the single point MP2 calculations are similar one to another, the MP2 association energies for species with piperidine were determined only on the basis of single point calculations. Both energies and geometries were also calculated by double hybrid B2PLYP method, which combines the exact HF exchange with a MP2-like correlation to a DFT.[36] Obtained association energies, $\Delta E[A{\cdot}nB]$, were corrected for the basis set superposition error (BSSE) and zero-point vibrational energy (ZPE). The BSSE was estimated using the counterpoise technique (CP).[37,38] In the case of MP2 association energy obtained from single point calculations, the ZPE corrections from DFT method were taken into account. The Gaussian 09 program package[39] was applied in the calculations.

DOI: 10.1021/acs.jpcb.6b10262
J. Phys. Chem. B 2017, 121, 3070−3086

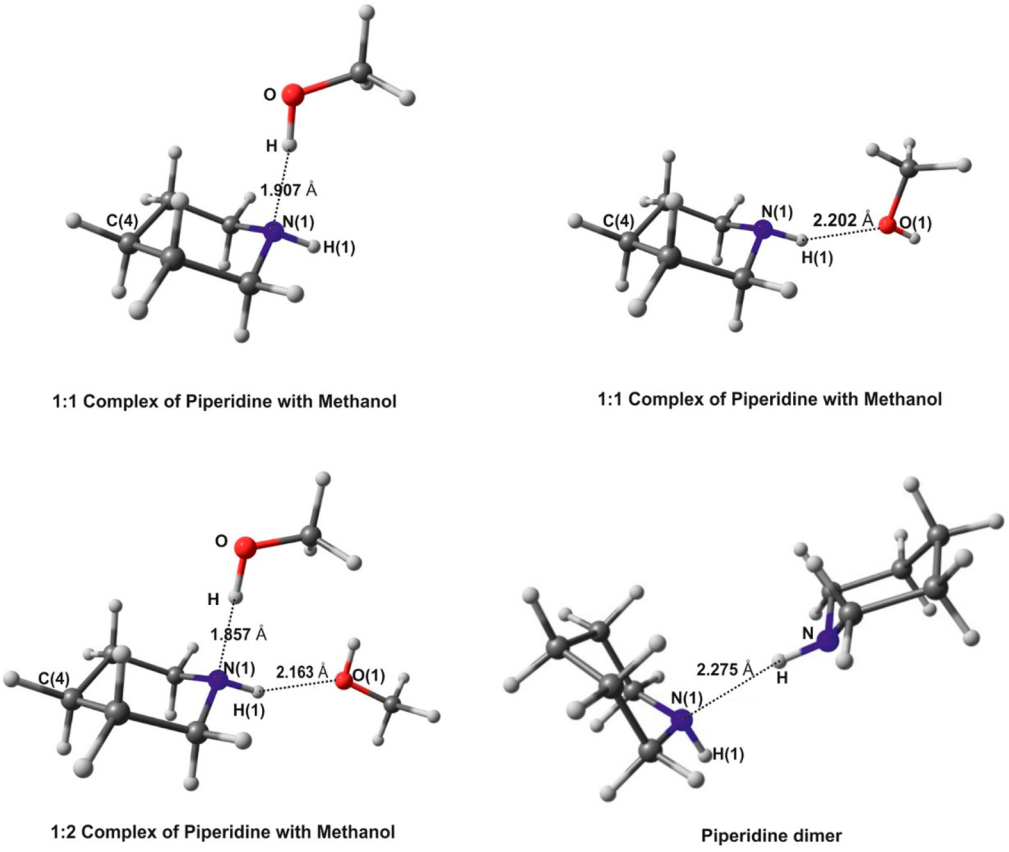

Figure 2. Optimized geometries of the piperidine−methanol complexes and of the piperidine dimer calculated by the B3LYP/aug-cc-pVDZ method. Bond lengths and valence angles reported in Supporting Information, Table S1. The piperidine dimer was reported earlier[2] and is shown here for the readers' convenience.

Optimized structures of molecular complexes obtained in the B3LYP/aug-cc-pVDZ calculations are presented in Figures 2 and 3, and relevant geometrical parameters are available as Supporting Information, Tables S1 and S2. Association energies are reported in Tables 1 and 2. As in the previous studies,[1,2,40−43] the following sequence of energies was observed: ΔE(MP2) > ΔE(B2PLYP) > ΔE(DFT/B3LYP). Lower B2PLYP and DFT/B3LYP values are due to underestimated dispersion energies which is a general feature of the DFT results.[44−46] For piperidine complex with methanol, two additional structures were considered (Figure 2, upper right and bottom left panel). One of them is a simple 1:1 complex with hydrogen bond of the N−H···O type, the second is a 1:2 complex containing two types of hydrogen bonds, i.e. O−H···N and N−H···O. According to the results collected in Table 2, the energies of N−H···O bond are about 2−3 times lower than those of O−H···N ones, depending on the method of calculation. Hydrogen bond of the N−H···O type is usually classified as weak[44,47,48] and from the point of view of energetics, creation of complexes with N−H···O bond is less favorable than creation of complexes with O−H···N bonds. Moreover, in case of the considered 1:1 piperidine−methanol N−H···O complex, the calculated association energies are also slightly lower than the ones calculated for the piperidine dimer with one N−H···N bond. The results of calculations for 1:2 piperidine−methanol complex show that the hydrogen bond cooperative effect is small. Both hydrogen bonds, O−H···N and N−H···O, are strengthened rather slightly, as the association energy increases only by about 2−3 kJ·mol^{-1} per bond in comparison with respective 1:1 complexes. Thus, in the light of the results discussed above, the most stable complexes among the considered theoretically structures are these with O−H···N bonds. Consequently, the formation of 1:1 complexes of the amines with methanol and water seems to be essential for the explanation of the studied systems properties, while that of 1:2 ones may play minor role.

3. EXPERIMENTAL SECTION

3.1. Chemicals. Pyrrolidine, *N*-methylpyrrolidine, piperidine, and *N*-methylpiperidine of mass fraction purity no less than 0.97 were purchased from Sigma-Aldrich. They were purified before usage by standard methodologies: dried with sodium and fractionally distilled under nitrogen atmosphere.[49] Anhydrous methanol was obtained by passage through Linde type 4 Å molecular sieves and further distillation. More detailed information about the chemicals is presented in Table 3.

Water was distilled twice and additionally deionized by an EasyPure II (Thermo Scientific) system. Its final resistivity was 18.2 MΩ·cm at 298.15 K. Heavy water (Sigma, 99.9% D_2O) and heavy methanol (Sigma, 99.8% CD_3OD) were used without any pretreatment.

Binary solutions were prepared by mass. The uncertainty in solutions mole fractions did not exceed 5×10^{-5}.

3.2. Apparatus. The solution enthalpies at temperature 298.15 ± 0.01 K were determined with the isothermal calorimeter TA Instruments TAM III, equipped with a titration input system which provided the solute injection in consecutive drops of the volume 5−20 μL into the thermostated glass cell

DOI: 10.1021/acs.jpcb.6b10262
J. Phys. Chem. B 2017, 121, 3070−3086

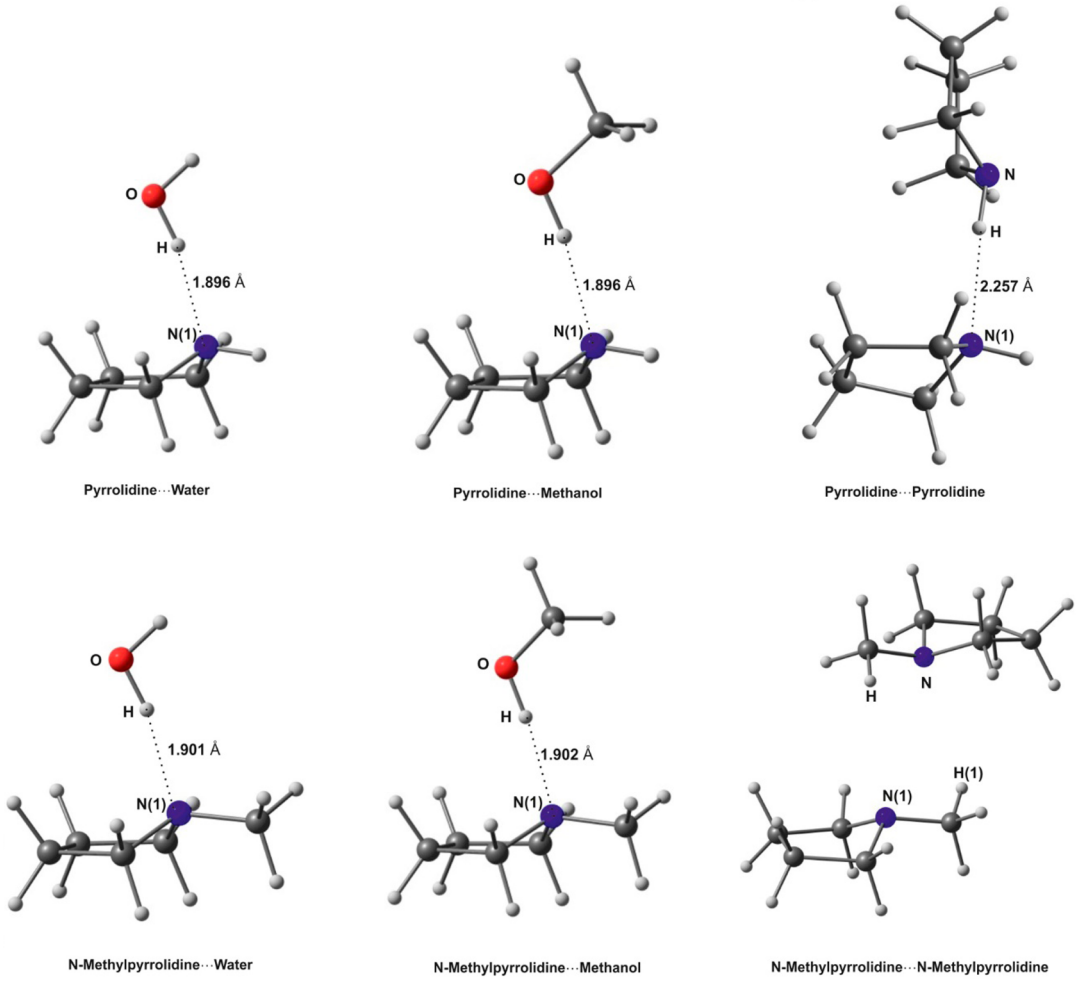

Figure 3. Optimized geometries of the complexes of pyrrolidine and *N*-methylpyrrolidine with water and methanol, and of pyrrolidine and *N*-methylpyrrolidine dimers. Structures obtained from the DFT/B3LYP/aug-cc-pVDZ calculations. Bond lengths and valence angles reported in Supporting Information, Table S2.

Table 1. Association Energies[a] of the 1:1 Complexes of Pyrrolidine and *N*-Methylpyrrolidine with Water and Methanol, and Those of the Pyrrolidine and *N*-Methylpyrrolidine Dimers[b]

		$(CH_2)_4NH$			$(CH_2)_4NCH_3$		
		H_2O	CH_3OH	$(CH_2)_4NH$	H_2O	CH_3OH	$(CH_2)_4NCH_3$
DFT/B3LYP	ΔE	30.6	30.1	12.3	29.5	28.8	4.7
	ΔE_{BSSE}	27.8	27.3	9.5	26.0	25.0	0.6
	$\Delta E_{BSSE+ZPE}$	19.5	21.7	7.0	17.8	19.2	−1.4
	$\Delta E_{BSSE+ZPE}$[c]	21.1	22.3		19.3	19.9	
MP2[d]	ΔE	39.8	42.2	26.4	40.1	43.5	20.3
	ΔE_{BSSE}	31.8	33.3	17.9	30.6	32.7	10.5
	$\Delta E_{BSSE+ZPE}$	23.4	27.6	15.5	22.4	26.9	8.4
	$\Delta E_{BSSE+ZPE}$[c]	25.0	28.3		23.9	27.6	
MP2	ΔE	41.0	43.8	34.6	42.2	46.6	32.9
	ΔE_{BSSE}	32.1	33.5	20.4	32.0	33.6	15.9
	$\Delta E_{BSSE+ZPE}$	23.3	28.0	17.5	23.3	28.3	13.3
	$\Delta E_{BSSE+ZPE}$[c]	25.1	28.7		25.0	29.0	
B2PLYP	ΔE	34.4	34.9	19.2	34.2	34.9	13.2
	ΔE_{BSSE}	30.0	30.1	13.1	28.9	29.0	5.8
	$\Delta E_{BSSE+ZPE}$	21.5	24.5	10.7	20.4	23.6	3.5
	$\Delta E_{BSSE+ZPE}$[c]	23.1	25.2		22.0	24.3	

[a] ΔE in kJ·mol^{-1} [b] BSSE, corrected for the basis set superposition error; ZPE, corrected for the zero-point vibrational energy. [c] Results for deuterated molecules: D_2O, CD_3OD. [d] Results obtained for single point calculations from the DFT/B3LYP optimized geometries.

DOI: 10.1021/acs.jpcb.6b10262
J. Phys. Chem. B 2017, 121, 3070−3086

Table 2. Association Energies[a] of the 1:1 and 1:2 Complexes of Piperidine with Methanol, and Those of the Piperidine Dimer[b]

		$(CH_2)_5NH{\cdot}CH_3OH$		$(CH_2)_5NH{\cdot}2CH_3OH$		$((CH_2)_5NH)_2$
		O−H···N	N−H···O	O−H···N	N−H···O	N−H···N
DFT/B3LYP	ΔE	29.7	10.3	34.3	14.9	12.5[c]
	ΔE_{BSSE}	26.8	8.7	29.7	11.7	9.1[c]
	$\Delta E_{BSSE+ZPE}$	20.2	5.8	22.9	8.6	6.4[c]
MP2[d]	ΔE	42.4	19.6	47.6	24.8	29.1[c]
	ΔE_{BSSE}	33.4	14.5	35.0	17.3	19.2[c]
	$\Delta E_{BSSE+ZPE}$	26.8	11.6	28.3	14.2	16.4[c]
B2PLYP	ΔE	34.7	14.3	39.2	18.8	19.6[c]
	ΔE_{BSSE}	29.8	11.0	32.0	14.3	13.0[c]
	$\Delta E_{BSSE+ZPE}$	24.1	7.8	26.1	10.9	10.8[c]

[a]ΔE in kJ·mol^{-1} [b]BSSE, corrected for the basis set superposition error; ZPE, corrected for the zero-point vibrational energy. [c]Reference2. [d]Results obtained for single point calculations from the DFT/B3LYP optimized geometries.

Table 3. Characteristics of the Chemicals Used in This Work

chemical	initial mass fraction purity	final mass fraction purity	analysis method	mass fraction of water[a]
methanol	0.98	0.998	GC	0.0003
pyrrolidine	0.99	0.997	GC	0.0002
N-methylpyrrolidine	0.97	0.995	GC	0.0004
piperidine	0.99	0.997	GC	0.0002
N-methylpiperidine	0.99	0.996	GC	0.0002

[a]As determined by the Karl Fischer titration.

filled with 100 mL of the solvent. The measurement procedure was described in detail earlier.[24,50] The instrument was checked on the basis of a test titration of propan-1-ol to water, which gave the solution enthalpy of −10.16 ± 0.03 kJ·mol^{-1} that agreed well with the recommended value of −10.16 ± 0.02 kJ·mol^{-1} reported by Hallén et al.[51]

The density and speed of sound were measured with an Anton Paar DSA 5000 apparatus with resolutions of 1 × 10^{-3} kg·m^{-3} and 1 × 10^{-2} m·s^{-1}, respectively. The accuracies were 5 × 10^{-2} kg·m^{-3} for the density and 5 × 10^{-1} m·s^{-1} for the speed of sound. The instrument was calibrated with water and dry air following the manufacturer's instructions. Measurement details were reported in the previous work.[52]

Small-angle neutron scattering experiments were performed on the Yellow Submarine instrument in the Budapest Neutron Center. The scattering vector q ranged from 0.4 to 4.3 nm^{-1}. The samples were placed in 2 mm thick quartz cuvettes, and thermostated during the scattering experiment at 298.15 K.

Table 4. Limiting Partial Molar Enthalpies of Solution, and Enthalpies of Hydrogen Bonding of Solutes (A) in Solvents (S) at T = 298.15 K and p = 0.1 MPa

		$\Delta_{soln}H^{A/S}$/(kJ·mol^{-1})		
solute (A)	solvent (S)	experimental	assessed[a]	$\Delta_{HB}H^{A/S}$/(kJ·mol^{-1})
$(CH_2)_4NH$	H_2O	−26.15 ± 0.02	−19.5 (−30.2)	−18.4[f]
		−26.12[b]		
$(CH_2)_5NH$	H_2O	−26.15 ± 0.02	−17.5[d] (−28.2)	−18.8[f]
		−26.14[b]		
$(CH_2)_4NCH_3$	H_2O	−30.15 ± 0.02	−17.8 (−28.5)	−22.0[f]
		−29.22[b]		
$(CH_2)_5NCH_3$	H_2O	−30.00 ± 0.01	−16.8[e] (−27.5)	−23.0[f]
		−30.00[b]		
		−30.08 ± 0.15[c]		
$(CH_2)_4NH$	CH_3OH	−13.34 ± 0.12	−13.9	−15.2
$(CH_2)_5NH$	CH_3OH	−13.30 ± 0.01	−12.4	−14.8
$(CH_2)_4NCH_3$	CH_3OH	−10.02 ± 0.01	−11.4	−10.1
$(CH_2)_5NCH_3$	CH_3OH	−10.38 ± 0.06	−10.5	−11.0
		−10.38 ± 0.03[c]		
H_2O	$(CH_2)_4NH$	−11.65 ± 0.04	−12.7	−38.7
H_2O	$(CH_2)_5NH$	−9.87 ± 0.02	−8.9	−36.3
H_2O	$(CH_2)_4NCH_3$	−2.10 ± 0.01	−2.4	−32.8
H_2O	$(CH_2)_5NCH_3$	−2.78 ± 0.11	−0.9	−33.3
CH_3OH	$(CH_2)_4NH$	−5.38 ± 0.03	−6.0	−21.1
CH_3OH	$(CH_2)_5NH$	−4.87 ± 0.01	−4.5	−20.0
CH_3OH	$(CH_2)_4NCH_3$	−3.06 ± 0.05	−3.5	−22.0
CH_3OH	$(CH_2)_5NCH_3$	−3.30 ± 0.11	−2.6	−22.1

[a]Assessed from the stabilization energies calculated by the DFT/B3LYP method; uncorrected values for water solvent obtained from eq 28, while the values in parentheses corrected for the hydrophobic effect from eq 29. [b]Reference 3. [c]Reference 53. [d]Reference 2. [e]Reference 1. [f]Corrected for the hydrophobic effect enthalpy (eq 7), equal to −10.7 kJ·mol^{-1}

DOI: 10.1021/acs.jpcb.6b10262
J. Phys. Chem. B 2017, 121, 3070−3086

Table 5. Coefficients a_i of eq 8 for Temperature Dependences of Densities of the Mixtures of *N*-Methylpyrrolidine with Water and of Pure *N*-Methylpyrrolidine in the Temperature Range 293.15−323.15 K, and Characteristics of the Fitting Quality δ_ρ

x_1	$a_0 \times 10^3$	$a_1 \times 10^4$	$a_2 \times 10^6$	$a_3 \times 10^8$	$\delta_\rho \times 10^6/(\mathrm{g\cdot cm^{-3}})$
0.010 62	6.4802	2.7173	4.8635	−1.9840	2
0.020 21	12.3517	3.5208	4.7116	−1.9721	1
0.030 21	16.2210	4.4170	4.2744	−1.9944	2
0.039 88	20.2049	5.3213	3.4491	−1.6914	3
0.050 69	22.5517	5.7669	2.7693	−0.7853	2
0.099 15	47.5642	8.1130	1.1293	1.2794	1
0.228 28	96.2909	10.0043	1.7027	0.6299	1
0.299 37	117.7438	10.5229	1.9784		3
0.398 80	141.5431	11.0019	1.6729	0.8750	2
0.497 93	162.4874	11.2869	1.8227	0.3251	1
0.599 75	180.7010	11.4906	1.7331	0.6375	2
0.699 17	195.6255	11.6649	1.9037		2
0.803 96	209.4598	11.8754	1.6978	0.2082	1
0.902 07	220.3196	12.0502	1.5837	0.1728	0
1.000 00	229.4709	12.1564	1.2134	0.5381	2

4. EXPERIMENTAL RESULTS

4.1. Limiting Partial Enthalpies of Solution and the Enthalpies of Hydrogen Bonding. Sixteen binary systems were studied: pyrrolidine, piperidine, *N*-methylpyrrolidine, and *N*-methylpiperidine in water and in methanol as well as water and methanol in the four amines. Calorimetric titrations were carried out for the solute concentration range in which the molar enthalpies of solution were constant, i.e. the maximum solute molality ranged from 13.2 to 113.5 mmol·kg^{-1} for *N*-methylpiperidine in water and water in *N*-methylpyrrolidine, respectively. The raw results are reported in the Supporting Information, Tables S3 and S4. Consequently, the limiting partial molar enthalpies of solution could be calculated as the arithmetic means of four to six experimental enthalpies of solution for each binary system. These mean values with standard deviations are reported in Table 4

Hydrogen bonding enthalpies were calculated by the Solomonov's method, using the following formula:[25]

$$\Delta_{HB}H^{A/S} = \Delta_{soln}H^{A/S} - \Delta_{soln}H^{A/C_6H_{12}} - (\delta_{cav}h^S - \delta_{cav}h^{C_6H_{12}})V^A_{char} - (a_R + b_R\sqrt{\delta_{cav}h^S}) \times [\Delta_{soln}H^{A/S_R} - \Delta_{soln}H^{A/C_6H_{12}} - (\delta_{cav}h^{S_R} - \delta_{cav}h^{C_6H_{12}})V^A_{char}] \quad (2)$$

Here $\Delta_{soln}H^{A/S}$, $\Delta_{soln}H^{A/S_R}$, $\Delta_{soln}H^{A/C_6H_{12}}$ are the solution enthalpies of solute A in solvent S, in standard solvent S_R, and in cyclohexane, respectively; $\delta_{cav}h^S$, $\delta_{cav}h^{S_R}$, and $\delta_{cav}h^{C_6H_{12}}$ are the specific relative cavity formation enthalpies for each solvent and $V_{char}{}^A$ is a characteristic volume of solute A.[54] $\delta_{cav}h^S$ is equal to the enthalpy of solution of linear alkane in the studied solvent S divided by the characteristic volume $V^{C_nH_{2n+2}}_{char}$ of the alkane:

$$\delta_{cav}h^S = \frac{\Delta_{soln}H^{C_nH_{2n+2}/S}}{V^{C_nH_{2n+2}}_{char}} \quad (3)$$

This value reflects the breaking of the solvent−solvent van der Waals interactions due to the dissolution of any solute molecule. Consequently, it can be applied as a relative measure of the solvent−solvent van der Waals interactions.

As in the previous study,[41] two standard solvents S_R were used: benzene for the proton acceptor solutes (a_R = 0.20, b_R = 0.38) and carbon tetrachloride for the proton donor ones (a_R = 0.34, b_R = 0.61). Data necessary for the calculations of $\Delta_{HB}H^{A/S}$ via eq 2 obtained in this study or reported in the literature[28−30,55] are attached as Supporting Information, Table S5.

The above formulas are valid provided the molecular state of the solute is the same in the gas phase as in the solution. In this study, we assumed that solutes are monomeric in both states.

Equation 2 is based on the idea that enthalpy of solvation of solute A in solvent S can be represented by a sum of the enthalpy of nonspecific solvation (van der Waals interaction term) and the enthalpy of specific interactions which includes contribution of donor−acceptor interactions, or a hydrogen bonding term:

$$\Delta_{solv}H^{A/S} = \Delta_{solv(nonsp)}H^{A/S} + \Delta_{int(sp)}H^{A/S} \quad (4)$$

In the case of water as a solvent, another contribution should be considered, which represents the enthalpy of the hydrophobic effect.[56−58] Consequently, the enthalpy of solvation of nonelectrolyte solute in water is given by the following equation:

$$\Delta_{solv}H^{A/S} = \Delta_{solv(nonsp)}H^{A/S} + \Delta_{int(sp)}H^{A/S} + \Delta_{h.e.}H^A \quad (5)$$

Since

$$\Delta_{solv}H^{A/S} = \Delta_{soln}H^{A/S} - \Delta^g_lH^A \quad (6)$$

where $\Delta^g_lH^A$ is the vaporization enthalpy of pure solute A, eq 2 could be transformed into eq 7 for the enthalpy of hydrogen bonding in aqueous solutions:

$$\Delta_{HB}H^{A/S} = \Delta_{soln}H^{A/S} - \Delta_{soln}H^{A/C_6H_{12}} - (\delta_{cav}h^S - \delta_{cav}h^{C_6H_{12}})V^A_{char} - (a_R + b_R\sqrt{\delta_{cav}h^S}) \times [\Delta_{soln}H^{A/S_R} - \Delta_{soln}H^{A/C_6H_{12}} - (\delta_{cav}h^{S_R} - \delta_{cav}h^{C_6H_{12}})V^A_{char}] - \Delta_{h.e.}H^A, \quad (7)$$

The enthalpy of hydrophobic effect is negative and approximately the same for various molecules of alkanes and their derivatives.[57,59] It was estimated for (−10.7 ± 1.5 kJ·mol^{-1}) for linear, cyclic and branched alkanes in water.[59] This value was used in the assessments of the hydrogen bonding

DOI: 10.1021/acs.jpcb.6b10262
J. Phys. Chem. B 2017, 121, 3070−3086

enthalpies of the aliphatic amines in water reported in the present work.

The enthalpies of hydrogen bonding calculated from eqs 2 and 7 are reported in Table 4. They should not be confused with the energy of the solute−solvent hydrogen bonds, because they result from both the formation and breaking of the hydrogen bonds due to the solvation. Thus, they represent enthalpy changes related to hydrogen bonding per 1 mol of the solute in the infinite amount of the solvent.

4.2. Excess Molar Volume and Isobaric Thermal Expansion. Densities of binary mixtures of *N*-methylpyrrolidine with water were measured for the full range of mole fractions in the temperature range 293.15−323.15 K. The experimental results are reported in Supporting Information, Table S6, with the number of significant digits corresponding to the measurements resolution because of the requirements of further calculations, especially those of the isobaric thermal expansibility. Dependences of the density (ρ) on temperature (T) were approximated by the following polynomials:

$$\ln(\rho/\mathrm{g\cdot cm^{-3}}) = -\sum_{i=0}^{3} a_i (T/\mathrm{K} - 298.15)^i \tag{8}$$

with the regression coefficients a_i obtained by the least-squares method, which are reported in Table 5, along with characteristics of the quality of fit:

$$\delta_\rho = \sqrt{\sum_j (\rho_{\mathrm{calc}} - \rho_{\mathrm{exp}})^2/(n-k)} \tag{9}$$

Here n and k are the numbers of experimental points and of a_i coefficients, respectively.

Since isobaric thermal expansibility is the temperature derivative of the density logarithm, $\alpha_p \equiv -(\partial[\ln \rho]/\partial T)_p$, it can easily be calculated from eq 8:

$$\alpha_p/\mathrm{K^{-1}} = \sum_{i=1}^{3} i a_i (T/\mathrm{K} - 298.15)^{i-1} \tag{10}$$

Excess molar volumes (V^{E}) and excess molar isobaric thermal expansions (E_p^{E}) were calculated from the thermodynamic relationships:

$$Z^{\mathrm{E}} = Z - \sum_{i=1}^{2} x_i Z_i^{\circ} \tag{11}$$

where $Z = V$ or $Z = E_p$, x is the mole fraction, subscript $i = 1$ for *N*-methylpyrrolidine and $i = 2$ for water, and superscript "°" denotes pure substance. Molar volume and molar isobaric thermal expansion are given by

$$V = \sum_{i=1}^{2} x_i M_i/\rho \tag{12}$$

and

$$E_p = \alpha_p V \tag{13}$$

where M_i is the molar mass. The experimental excesses are reported in Supporting Information Table S7.

The dependence of excess molar volume on concentration and temperature was approximated by the modified Redlich−Kister polynomial:

$$V^{\mathrm{E}}/(x_1x_2) = \sum_{i=0}^{2}\sum_{j=0}^{4} a_{ij}\vartheta^i (x_2 - x_1)^j \tag{14}$$

where $\vartheta = T/\mathrm{K} - 298.15$, and a_{ij} are regression coefficients. Since the excess molar volume depends much stronger on concentration than on temperature, conventional least-squares fitting of eq 14 with a stepwise rejection of statistically insignificant regression coefficients gave rather unreliable sets of a_{ij} coefficients, which was evidenced by significant differences between E_p^{E} values obtained directly from eq 13 and by the temperature derivatives of eq 14:

$$E_p^{\mathrm{E}} = (\partial V^{\mathrm{E}}/\partial T)_p \tag{15}$$

To overcome this difficulty, the fitting procedure was performed in four steps: (i) provisional regression coefficients were calculated for seven isotherms (approximately 293.15, 298.15, and so on up to 323.15 K); (ii) statistically insignificant regression coefficients were rejected on the basis of *F*-test results; (iii) temperature dependences of the significant coefficients were found to be parabolic; (iv) eq 14 with 12 a_{ij} coefficients selected in the above manner was fitted to the experimental excess volumes by the least-squares method. The correlation coefficient was equal to 0.9994. The a_{ij} coefficients are reported in Table 6, and the $V^{\mathrm{E}}_{T=\mathrm{const.}}(x_1)$ curves are plotted in Figure 4. A comparison of the excess molar thermal expansions calculated according to eq 13 with the Redlich−Kister polynomial derivatives eqs 14 and 15 are presented in Figure 5.

Table 6. Coefficients of Eq 14 for the Excess Molar Volume[a] of *N*-Methylpyrrolidine + Water in the Temperature Range 293.15−298.15 K at Pressure p = 0.1 MPa

j	$a_{0j} \times 10^6$	$a_{1j} \times 10^8$	$a_{2j} \times 10^{10}$
0	−7.5378	0.526 54	0.244
1	−2.8943	2.082 46	−1.862
3	−1.8846	−0.571 32	−2.361
4	−2.2126	2.627 95	−1.763

[a] V^{E} in $\mathrm{m^3\cdot mol^{-1}}$

4.3. Speed of Ultrasound and Isentropic Compressibility. Speeds of ultrasound, u, in dilute solutions of *N*-methylpyrrolidine were measured in the temperature range from 293.15 to 323.15 K, in 5 K intervals. Isentropic compressibilities, κ_S, were calculated from the Laplace formula:

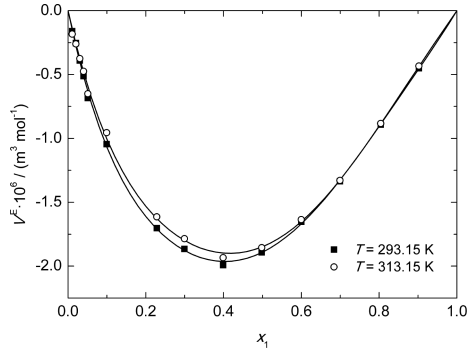

Figure 4. Excess molar volume of binary system *N*-methylpyrrolidine + water. Points, experimental results; lines, eq 14.

DOI: 10.1021/acs.jpcb.6b10262
J. Phys. Chem. B 2017, 121, 3070−3086

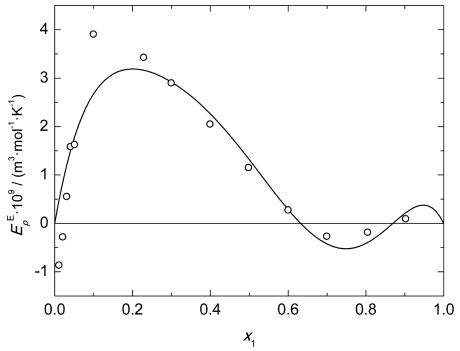

Figure 5. Excess molar isobaric thermal expansion of binary system *N*-methylpyrrolidine + water at T = 298.15 K. Points, experimental results; line, eq 15 with V^E given by eq 14.

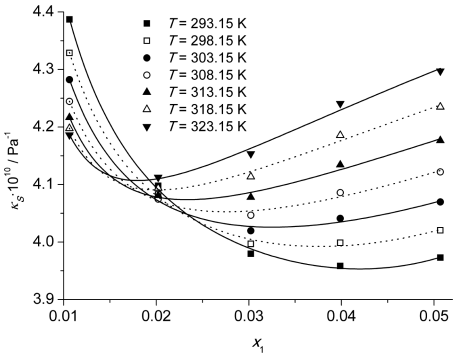

Figure 6. Isentropic compressibility of aqueous solutions of *N*-methylpyrrolidine. Points, experimental results; lines, fitted empirical equation $\kappa_S = k_0(1 - x_1)/x_1 + k_1x_1^n + k_2$, where k_i and n are the regression coefficients.

$$\kappa_S = (\rho u^2)^{-1} \tag{16}$$

The results are reported in Table 7 and plotted in Figure 6.

4.4. Small-Angle Neutron Scattering (SANS). Neutron scattering was recorded for five mixtures of *N*-methylpyrrolidine with D_2O, with mole fraction x_1 ranged from 0.036 to 0.215, and for mixtures of pyrrolidine with D_2O, for x_1 from 0.049 to 0.344. The coherent small-angle scattering signal evidence that the studied mixtures are heterogeneous on the nanometer length scale, similarly as those of *N*-methylpiperidine[1] and piperidine[2] with D_2O.

Three solutions of lower *N*-methylpyrrolidine mole fraction (x_1 = 0.036, 0.047, and 0.071) show enhanced forward scattering, which was successfully modeled by the Ornstein–Zernike function for the concentration fluctuations:

$$I = \frac{I_0}{1 + q^2\xi^2} + I_{bg} \tag{17}$$

where q is the scattering vector, I_0 is the magnitude of the q-dependent coherent forward scattering intensity at q = 0, ξ is the correlation length of the fluctuations in the scattering length density, and I_{bg} is the constant background term. Values of ξ, calculated by the weighted least-squares method, are reported in Table 8.

The scattering in solutions with *N*-methylpyrrolidine mole fraction 0.095 and 0.215 was well-approximated by the Teubner–Strey function, which describes a microphase separated system with two characteristic lengths:[60,61]

$$I = \frac{1}{a + c_1q^2 + c_2q^4} + I_{bg} \tag{18}$$

Here a, c_1, and c_2 are fitting coefficients related to the quasi-periodic repeat distance D (or first neighbor distance) and the decay length of the correlations ξ by the following equations:

$$D = 2\pi\left[\frac{(a/c_1)^{1/2}}{2} - \frac{c_1}{4c_2}\right]^{-1/2} \tag{19}$$

$$\xi = \left[\frac{(a/c_1)^{1/2}}{2} + \frac{c_1}{4c_2}\right]^{-1/2} \tag{20}$$

The characteristic lengths D and ξ, calculated from a, c_1, and c_2 coefficients obtained by the weighted least-squares method, are reported in Table 8, and the scattering curves are plotted in Figure 7. Unfortunately, the estimates of the a, c_1, and c_2 standard deviations did not converge in the calculations for the mixture of x_1 = 0.2149. Thus, we assumed the uncertainties of D and ξ equal to those calculated for the mixture of x_1 = 0.0948. The nonlinear least-squares fit with user-defined loss function module of Statistica 12 software[62] was applied in the calculations.

The Fourier transform of the scattering intensity, given by eq 18, yields the correlation function of the scattering length density in the real space:[61]

Table 7. Speed of Ultrasound in and Isentropic Compressibility of Dilute Solutions of *N*-Methylpyrrolidine in Water in the Temperature Range 293.15–323.15 K

	T/K						
x_1	293.15	298.15	303.15	308.15	313.15	318.15	323.15
				u/(m·s^{-1})			
0.010 62	1513.76	1524.86	1534.25	1542.38	1548.93	1554.10	1557.97
0.020 21	1570.51	1574.75	1577.72	1579.46	1580.03	1579.52	1578.00
0.030 21	1596.42	1594.65	1591.97	1588.65	1584.68	1580.06	1574.79
0.039 88	1603.47	1597.43	1591.22	1584.80	1577.89	1570.69	1563.02
0.050 69	1602.23	1595.01	1587.65	1579.98	1572.13	1563.89	1555.18
				$\kappa_S \times 10^{10}$/Pa^{-1}			
0.010 62	4.386 96	4.328 68	4.282 17	4.244 40	4.216 66	4.197 52	4.186 32
0.020 21	4.097 99	4.082 64	4.074 92	4.074 49	4.080 94	4.093 76	4.112 62
0.030 21	3.979 61	3.996 79	4.019 56	4.046 54	4.077 82	4.113 46	4.153 57
0.039 88	3.958 55	3.998 81	4.041 18	4.085 82	4.134 31	4.185 59	4.240 79
0.050 69	3.973 05	4.020 38	4.069 76	4.122 06	4.176 70	4.234 92	4.297 28

DOI: 10.1021/acs.jpcb.6b10262
J. Phys. Chem. B 2017, 121, 3070–3086

Table 8. Quasi-Periodic Repeat Distance D, and the Decay Length of the Correlations ξ, in the Mixtures of N-Methylpyrrolidine with D_2O

x_1	φ_1[a]	model	D/nm	ξ/nm
0.0357	0.1793	Ornstein−Zernike eq 17	–	0.306 ± 0.014
0.0468	0.2244	Ornstein−Zernike eq 17	–	0.331 ± 0.011
0.0706	0.3094	Ornstein−Zernike eq 17	–	0.322 ± 0.012
0.0948	0.3819	Teubner−Strey eqs 18, 19 and 20	3.09 ± 0.14[b]	0.443 ± 0.021[b]
0.2149	0.6176	Teubner−Strey eqs 18, 19 and 20	2.16 ± 0.14[c]	0.563 ± 0.021[c]

[a]Volume fraction of N-methylpyrrolidine. [b]Uncertainty estimated from standard deviations of the coefficients a, c_1, and c_2 in eq 18 [c]Approximate uncertainty assumed to be equal to that assessed for the mixture of x_1 = 0.0948

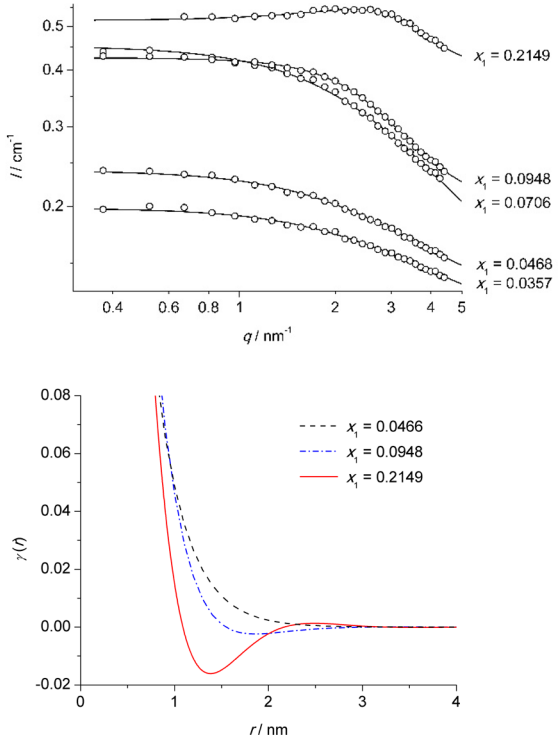

Figure 7. (Top) SANS curves for N-methylpyrrolidine + D_2O mixtures at T = 298.15 K. Points, experimental results; lines, Ornstein−Zernike eq 17 for x_1 = 0.0357, 0.0468, and 0.0706, and Teubner−Strey eq 18 for x_1 = 0.0948, and 0.2149. (Bottom) Real-space correlation functions eq 21 (two lines are omitted for the clarity of presentation).

$$\gamma(r) = \frac{\sin(2\pi r/D)}{2\pi r/D} \times \exp\left(-\frac{r}{\xi}\right) \tag{21}$$

In mixtures of protiated organic molecules with heavy water, the scattering length density correlates with the local composition on the nanometer length scale. Assuming that the mixture consists of two phases—aggregates, rich in solute, and the solvent phase containing less solute molecules—the minimum of the correlation function reflects the characteristic distance between the two dislike domains, and the following maximum shows the probable separation between the similar domains, as illustrated in Figure 7. The characteristic distance between the aggregates is seen to be about 2.5 nm, for the highest amine concentration x_1 = 0.2149, and only a shallow minimum is seen for x_1 = 0.0948. For the concentrations $x_1 \leq$ 0.0706, the correlation function is an exponential decay, characteristic of random concentration fluctuations. It can be noted, that although we used here eqs 17 and 18 to calculate the correlation function, the perfect agreement between the models and the data implies that the resulting correlation functions are nearly model-independent, and reflect the true structure of the studied mixtures, with the usual limitations inherent to the SANS technique.

Contrary to aqueous solutions, seven mixtures of N-methylpyrrolidine with CD_3OD (x_1 range from 0.021 to 0.538) show the scattering intensity independent of the scattering vector. The mixtures of pyrrolidine with D_2O show the coherent small-angle scattering signal for x_1 from 0.049 to 0.344. However, the results obtained in this experiment proved to be insufficient for reliable model fitting because of the weak coherent scattering signal.

5. DISCUSSION

Limiting partial molar enthalpies of solution could be estimated from the theoretically calculated aggregation energies applying an approach similar to that suggested in the earlier work.[1] The approach is based on the following assumptions: (i) the formation of the solute−solvent cross-associates and breaking of the molecular aggregates which occur in pure liquids are revealed in the enthalpy of solution, (ii) the solute molecules are solvent-separated one from another at infinite dilution, (iii) energies of binary molecular interactions are sufficient to account for the enthalpy effects of solution and co-operative effects are not considered. Consequently, a series of chemical reactions can be suggested for the solution and the overall heat effect can be calculated according to Hess' law. Obviously, the model is considerably simplified mainly due to the assumption iii, which is appropriate for gases rather than for liquids. It could be expected that more sophisticated models with multiple interactions will give better results. On the other hand, they have to account for more than just one physicochemical property of the mixture.

5.1. Dissolution of the Amines in Methanol. Exothermic effects of dissolution in methanol can be explained by the formation of 1:1 complexes according to the following chemical reaction:

$$(CH_3OH)_b + RN \xrightarrow{\Delta H_1} CH_3OH + RN \xrightarrow{\Delta H_2} CH_3OH\cdots NR \tag{22}$$

where subscript "b" denotes "bonded molecule" which is incapable of acting as a donor of proton, because the latter is already involved in hydrogen bond between two methanol molecules. Since molecules of methanol may form chains of different length or even closed loops in pure liquid phase,[63] the enthalpy change ΔH_1 can be estimated in the manner suggested in our previous work.[41] Only free hydroxyl group of the alcohol molecule (i.e., the terminal one in a chain) is capable of O−H···N bonding with the amine molecule. Energy equal to $k\Delta E[(CH_3OH)_2]$ per 1 mol of pure methanol must be supplied for its complete dissociation, i.e., the transformation

DOI: 10.1021/acs.jpcb.6b10262
J. Phys. Chem. B 2017, 121, 3070−3086

into isolated CH_3OH molecules. Here, $\Delta E[(CH_3OH)_2]$ is given by eq 1, and the coefficient k is related to the average association number of bulk methanol n by the following formula:

$$k = (n - 1)/n \tag{23}$$

Here $n = 2$ for dimers, $n = 3$ for trimers, *etc.*, up to $n = \infty$ for the chains of infinite length and cyclic aggregates without side branches. Thus

$$\Delta H_1 = k\Delta E[(CH_3OH)_2] \tag{24}$$

where $0.5 \leq k \leq 1$.

The enthalpy change due to the formation of the cross-associates (complexes) can be approximated by the negative stabilization energy of the methanol−amine complex:

$$\Delta H_2 = -\Delta E[RN{\cdot}CH_3OH] \tag{25}$$

Here $\Delta E[RN{\cdot}CH_3OH]$ is defined by eq 1. Eventually

$$\Delta H = \Delta H_1 + \Delta H_2 = k\Delta E[(CH_3OH)_2] - \Delta E[RN{\cdot}CH_3OH] \tag{26}$$

Enthalpies ΔH estimated by the above method from the DFT/B3LYP energies were collected in Table 4. Data for *N*-methylpiperidine were taken from the previous work.[1] Since $\Delta E[(CH_3OH)_2]$ was not calculated by the DFT/B3LYP method, the MP2 value of 15.7 kJ·mol^{-1} was used in the calculations. The agreement with the experimental enthalpies is fairly good assuming $k = 0.5$ for the DFT/B3LYP and B2PLYP energies, while $k = 1$ is suitable for the MP2 ones. This discrepancy evidence that association numbers n, which determine the k values, can be assessed only roughly from eq 26.

The good agreement was achieved in spite of the neglected effects of the N−H···N bonds breaking upon the solution of pyrrolidine and piperidine in methanol. Indeed, pure pyrrolidine and piperidine are associated liquids due to these bonds, as is evidenced by relatively high stabilization energies of the dimers especially in comparison with those for *N*-methylpyrrolidine (Tables 1 and 2). The aggregates in pure liquids are probably remnants of the N−H···N bonded chains in pyrrolidine[12,13] and piperidine[14] crystals. In crystalline hydrates of pyrrolidine, however, N−H···O bonds occur beside the stronger O−H···N bonds.[21] The former may be present in the liquid solutions in methanol, the more so because there is just one hydrogen atom in methanol molecule capable of forming O−H···X bonds, while two such atoms are in that of water. Thus, the positive enthalpy of the N−H···N bonds breaking upon solution would be compensated by the negative effect of the N−H···O bonds formation. Consequently, a reliable separation of the two shares in the limiting partial enthalpy of solution is impossible in the present approach. That explains also why absolute values of the specific interaction enthalpies of methanol with pyrrolidine and piperidine are higher than of those involving the *N*-methyl-substituted derivatives. Similar differences, although smaller, are in the values of the limiting partial molar enthalpies of solution (cf. Table 4).

5.2. Dissolution of the Amines in Water. The limiting partial enthalpies of solution of the four amines in water are from two to three times bigger than those in methanol (Table 4), in spite of lower stabilization energies of the complexes with water (cf. Tables 1 and 2, and ref.[1]). Differences between the energies for complexes with water and methanol range from 7% (*N*-methylpyrrolidine, DFT/B3LYP) to 18% (piperidine, MP2). The concentration of free hydroxyl groups seems to be higher in pure water than in methanol, because each molecule of water has two protons able to participate in hydrogen bonds, while just one such proton is in that of methanol. Consequently, the complex formation would not require breaking of the O−H···O bonds between water molecules, and the following chemical reaction may be sufficient to describe this process:

$$H_2O + RN \xrightarrow{\Delta H} HOH{\cdots}NR \tag{27}$$

Here

$$\Delta H = -\Delta E[RN{\cdot}H_2O] \tag{28}$$

where $\Delta E[RN{\cdot}H_2O]$ is defined by eq 1. The chemical formula H_2O in eq 28 is not to be confused with free, i.e., "monomeric" water molecule. It is sufficient that the molecule has one free proton capable of hydrogen bonding. Note that the DFT/B3LYP stabilization energies are close to the thermodynamic values of the hydrogen bonding enthalpies in aqueous solution (cf. Table 4). The difference is about 1 kJ·mol^{-1} for pyrrolidine and piperidine and about 4−5 kJ·mol^{-1} for the methyl derivatives. Consequently, the solution enthalpies of the amines in water assessed form the DFT/B3LYP energies via eq 28 significantly differ from the measured solution enthalpies, because the strengthening of the water−water O−H···O bonds in the vicinity of the O−H···N ones has not been considered in the calculations. The differences are 6.6, 8.6 12.4, and 13.2 kJ·mol^{-1} for pyrrolidine, piperidine, *N*-methylpyrrolidine and *N*-methylpiperidine, respectively. As suggested by the $\Delta_{HB}H^{A/S}$ values reported in Table 4, the effects would be bigger for the methyl-substituted derivatives, which are more hydrophobic than their nonsubstituted counterparts. The mean difference of 10.2 kJ·mol^{-1} is in perfect agreement with the $\Delta_{h.e.}H^{A}$ value estimated by the thermodynamic method for (−10.7 ± 1.5) kJ·mol^{-1}.[46] Thus, eq 25 could be modified, by analogy with eqs 2 and 7, as follows:

$$\Delta H = -\Delta E[RN{\cdot}H_2O] + \Delta_{h.e.}H^{A} \tag{29}$$

where $\Delta_{h.e.}H^{A} = -10.7$ kJ mol^{-1}. The limiting partial molar enthalpies of solution of the four amines in water, calculated from eq 29, are in good agreement with the experimental data (cf. Table 4).

5.3. Dissolution of Methanol in the Amines. Dissolution of methanol in pyrrolidine, piperidine, *N*-methylpyrrolidine and *N*-methylpiperidine may be discussed in terms of chemical reaction given by eq 22. The only difference is that methanol aggregates dissociate completely, and individual methanol molecules are separated one from another by the amine solvent. Consequently, k coefficient in eq 26 would be close to 1. A comparison of the limiting partial enthalpies of solution estimated in this manner with $k = 1$ with the experimental values, evidence that the DFT/B3LYP energies lead to almost quantitative agreement (Table 4). The agreement for MP2 and B2PLYP energies is qualitative—in both cases, an exothermic effect of dissolution is predicted.

5.4. Dissolution of Water in the Amines. Slightly more complicated model accounts for the observed limiting partial enthalpies of solution of water in the four amines. Similarly as for the dissolution of methanol, the individual molecules of water are assumed to be solvent-separated in the solution.

DOI: 10.1021/acs.jpcb.6b10262
J. Phys. Chem. B 2017, 121, 3070−3086

Thus, the dissolution consists in "monomerization" of water followed by the cross-association

$$(H_2O)_b + mRN \xrightarrow{\Delta H_1} H_2O + mRN \xrightarrow{\Delta H_2} (RN)_m \cdot H_2O \quad (30)$$

where

$$\Delta H_1 = 2\Delta E[(H_2O)_2] \quad (31)$$

upon the assumption that two hydrogen bonds must be broken to release one water molecule, and

$$\Delta H_2 = -m\Delta E[(RN)_m \cdot H_2O] \quad (32)$$

where $\Delta E[(H_2O)_2]$ and $\Delta E[(RN)_m \cdot H_2O]$ are defined by eq 1, with $m = 1$ and $m = 2$ for the formation of 1:1 and 2:1 amine–water complexes, respectively. Thus:

$$\Delta H = 2\Delta E[(H_2O)_2] - m\Delta E[(RN)_m \cdot H_2O] \quad (33)$$

Steric hindrance for hydrogen bonding constituted by methyl group at the nitrogen atom causes that the average ratio of amine to water molecules is probably lower for the complexes with methyl substituted amines. Indeed, the limiting partial enthalpies of solution calculated from the DFT/B3LYP energies remain in good agreement with the experimental results for $m \approx 1.5$ for *N*-methylpyrrolidine and *N*-methylpiperidine and $m \approx 1.9$ for pyrrolidine and piperidine (cf. Table 4). Slightly different values of m were estimated from the MP2 energies: 1.2 and 1.5, and from the B2PLYP energies: 1.3 and 1.7, respectively. The discrepancies in the m values obtained from different energies seem to be acceptable taking into account considerable uncertainties in the stabilization energies. For example, estimates of the binding energy of $(H_2O)_2$, are rather scattered, e.g., 9.5 kJ·mol^{-1} [44] and 12.17 kJ·mol^{-1},[64] obtained by the MP2 method with BSSE and ZPE corrections. Experimental method of velocity map imaging and resonance-enhanced multiphoton ionization gave the value of 13.2 ± 0.12 kJ·mol^{-1}, which was in perfect agreement with that calculated at the CCSDT(T)/aug-ccpVTZ level of theory.[65] Independently of the theoretical energies applied in the calculations (DFT/B3LYP, B2PLYP, or MP2), the values of m for the two secondary amines are by 25–30% higher than those for the two tertiary ones.

5.5. Correlation of the Calculated Enthalpies with the Experimental Values. Correlation of the experimental limiting partial molar enthalpies of solution with those based on the DFT/B3LYP theoretical estimations is satisfactory, which is evidenced by the correlation coefficient $r = 0.990$ for the regression equation:

$$\Delta H(\text{theor}) = a\Delta_{soln}H^{A/S} \quad (34)$$

with $a = 1.01 \pm 0.03$. An illustration is given in Figure 8. Thus, mainly binary interaction energies influence the limiting enthalpies of solution for the amines in methanol and *vice versa*, as well as for water in the four amines. However, the hydrophobic hydration must be considered in the case of dissolution of the amines in water.

5.6. Mixtures of Finite Concentrations: Small-Angle Neutron Scattering, Thermodynamic Excess Functions, And Isentropic Compression. The discussion of enthalpies dealt with infinitely dilute solutions. Molecular aggregation due to hydrogen bonds is manifested in the properties of mixtures at finite concentrations.

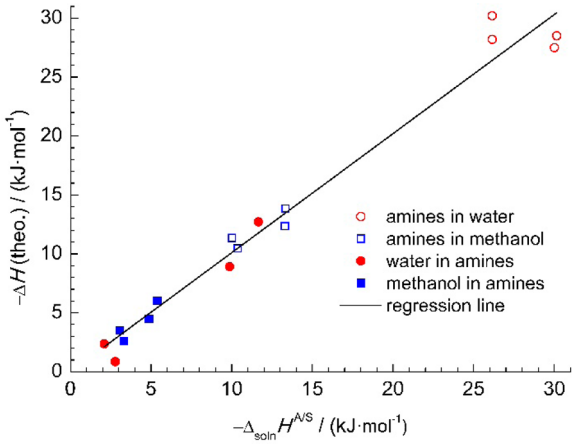

Figure 8. Correlation of the experimental limiting partial molar enthalpies of solution with the DFT/B3LYP-based theoretical estimations.

Aqueous solutions of *N*-methylpyrrolidine with mole fraction up to 0.071 show enhanced forward scattering which was successfully modeled by the Ornstein–Zernike type of scattering function (Figure 7), similarly to those of *N*-methylpiperidine.[1] Such scattering is typical of concentration fluctuations.[66−68] At higher concentrations of *N*-methylpyrrolidine, for $x_1 = 0.094$ and 0.215, the scattering curves gradually change their form from a Lorentzian centered at zero scattering angle, to a distinct interference peak at a finite angle. This shape is well-known in SANS data on microemulsions consisting of surfactant-separated water and oil phases. In the present case, however, in the absence of fully hydrophobic molecules, and in accordance with the amphiphile character of *N*-methylpyrrolidine, the solutions are seen to be microphase separated on the molecular level, with a characteristic interdomain distance of about 2 nm. A possibly similar picture of structural organization has been demonstrated recently in computer simulations of concentrated TBA–water solutions by Perera et al., who introduced the concept of molecular emulsions for aqueous mixtures of small organic molecules, exhibiting structural heterogeneity, which is distinct from statistical concentration fluctuations.[69−71] Similar scattering curves of the Teubner–Strey form were also reported for the solutions of piperidine in D_2O, for the amine mole fraction range from 0.044 to 0.588.[2] Thus, a propensity to molecular segregation on the nanometer scale in the aqueous solutions of the studied amines decreases in the following order: piperidine > *N*-methylpyrrolidine > *N*-methylpiperidine. The segregation in the solutions of pyrrolidine is probably stronger than in those of piperidine.

Unlike in aqueous solutions, the neutron scattering intensity is independent of the scattering vector for the solutions of *N*-methylpyrrolidine in deuterated methanol, evidencing that the latter are homogeneous in the nanometer-length scale. Similar result was obtained for *N*-methylpiperidine in methanol.[1] That supports the idea of amine–water complexes aggregation due to hydrogen bonds between the hydration water molecules sketched in Figure 9, similar to that suggested for aqueous solutions of pyridine and its methyl derivatives.[23]

Certainly, substitution of H_2O by D_2O in binary mixtures, necessary for technical reasons in SANS experiments, changes somewhat the enthalpy–entropy balance because deuterium bonds are stronger than protium ones; the O–D···O bond energy in pure water is higher than the O–H···O one by 929 J·

DOI: 10.1021/acs.jpcb.6b10262
J. Phys. Chem. B 2017, 121, 3070–3086

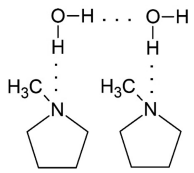

Figure 9. O–H···O bond between hydration water molecules suggested to account for the aggregation of *N*-methylpyrrolidine–water complexes.

mol^{-1},[72] and the stabilization energies of the studied complexes of amines with D_2O are by ca. 1 kJ·mol^{-1} (i.e., 7–8%) higher than of those with H_2O (cf. Table 1). However, the enthalpies of mixing, in which multimolecular interactions are revealed, are probably approximately independent of the isotopic composition of water at least at temperatures and pressures sufficiently distant from that of the critical decomposition, as was confirmed experimentally for binary mixtures of methylpyridine isomers with water.[73] Consequently, similar molecular aggregates probably occur in the mixtures with H_2O and D_2O.

X-ray diffraction and Raman spectroscopy studies of solids evidenced that pyrrolidine hexahydrate forms semiclathrates in which single pyrrolidine molecule is O–H···N and N–H···O bonded to water polyhedron enclosing its hydrophobic part.[21] Such clathrate-like structures may occur in liquid aqueous solutions of pyrrolidine and of the three other amines. This generalization is justified by the fact that piperidine and *N*-methylpiperidine form solid clathrate hydrates of type sII[20] and sH,[15] respectively, in the presence of methane at elevated pressures. Obviously, the reinforcement of water structure would be particularly significant in the vicinity of nitrogen atom due to cooperative effects. This probably leads to high exothermic effects of hydrogen bonding upon solution reported in Table 4.

An important difference between solid clathrates and clathrate-like structures in liquids consists in significant disruption of water polyhedra in the latter. With increasing temperature, the hydrogen-bonded network gradually decays that may lead to phase separation, as in the *N*-methylpiperidine–water system which shows lower critical solution temperature (LCST) of 316.7 K at the amine mole fraction 0.06 ± 0.01[1] (LCST 315 K at 0.07[74]). The O–H···O bonds that are farther from the O–H···N ones break as the first, while the water-amine complexes remain still linked one to another by the hydrogen bonds between water molecules. An increase of the amine concentration in mixtures with water may also cause breaking of the clathrate-like polyhedra. That would lead to microheterogeneities in the mixture, manifested in the intensity of small-angle neutron scattering in aqueous solutions of *N*-methylpyrrolidine (Table 8), piperidine,[2] and *N*-methylpiperidine.[1] Coherent small-angle scattering signal obtained in our preliminary studies of pyrrolidine in D_2O, not reported in this work because of rather low quality results, suggested that these mixtures were also heterogeneous on the nanometer length scale.

Negative excess molar volume of the system *N*-methylpyrrolidine–water is approximately equal to that of *N*-methylpiperidine–water and distinctly bigger than those of pyrrolidine–water and piperidine–water systems (Figure 10). That is in spite of slightly lower stabilization energies of the 1:1 amine–water complexes for methyl-substituted amines in comparison with the nonsubstituted ones (cf. $\Delta E_{BSSE+ZPE}$ values reported for pyrrolidine and *N*-methylpyrrolidine in

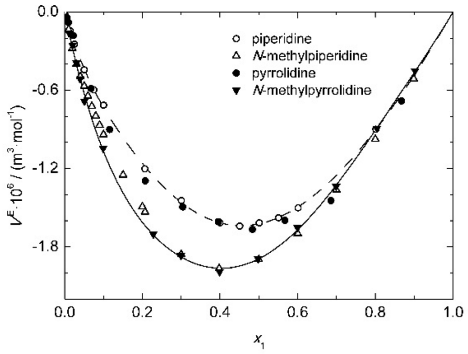

Figure 10. Excess molar volumes of binary mixtures of pyrrolidine,[5] *N*-methylpyrrolidine (this work), piperidine,[2] and *N*-methylpiperidine[1] with water at T = 298.15 K. Points, experimental results; lines, eq 14 for the system with *N*-methylpyrrolidine and an empirical function[2] for that with piperidine. Curves for the two other systems were omitted for the picture clarity.

Table 1, and those of 17.5, 21.9, and 20.3 kJ·mol^{-1} for piperidine and 16.8, 24.0, 20.0 kJ·mol^{-1} for *N*-methylpiperidine, calculated by the DFT/B3LYP, MP2 and B2PLYP, respectively).[1,2] Substantial difference between the excess volumes of binary mixtures of water with nonsubstituted and methyl-substituted amines is probably due to breaking of the amine–amine N–H···N bonds that accompanies dissolution of the former. This undoubtedly causes an increase of the volume which partially compensates for its decrease due to the formation of the O–H···N bonds. Differences in the excess volumes may also be attributed to the differences in shape of the molecules, which result in various packing of the molecules in pure liquids and solutions. The size of molecules seems to be less important, as the excesses for the five- and six-membered ring compounds belonging to the same subcategory of secondary or tertiary amines do not differ one from another.

Excess molar thermal expansions of binary systems pyrrolidine–water (calculated from the excess volumes reported by Álvarez et al)[5] and *N*-methylpyrrolidine–water (measured in this study) are positive in the amines mole fraction range from ca. 0.025 to 0.6. In this respect, they differ from those of the mixtures of piperidine[2] and *N*-methylpiperidine[1] with water, which show positive E_p^E values in the whole concentration range except for the mole fractions below 0.015 (Figure 11). The negative E_p^E at low x_1 is most probably due to structures formed by hydrogen-bonded water molecules around the amine ones. Analysis of well-known thermodynamic relationship

$$E_p^E = -(\partial S^E/\partial p)_T \quad (35)$$

where S^E is excess entropy, supports that supposition. The hydration polyhedra would be gradually destroyed with increasing pressure (similarly as the structure of ice Ih in the pressure-induced melting of water), that would effect in the increase of entropy exceeding that for thermodynamic ideal mixture. Consequently, $(\partial S^E/\partial p)_T > 0$ and $E_p^E < 0$.

Positive excess molar expansion at concentrations x_1 above 0.015 for piperidines and above 0.025 for pyrrolidines (Figure 11), i.e., $(\partial S^E/\partial p)_T < 0$ suggests that pressure favors aggregation of XN·H_2O complexes through O–H···O bonds between the hydration water molecules. Microheterogeneities in the liquid may expand and, eventually, the system may split into two phases at sufficiently high pressures. Such pressure-

DOI: 10.1021/acs.jpcb.6b10262
J. Phys. Chem. B 2017, 121, 3070–3086

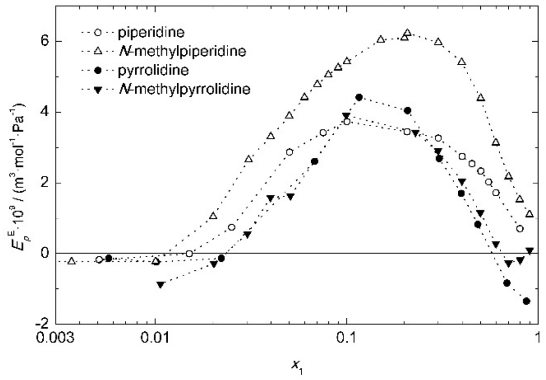

Figure 11. Excess molar isobaric thermal expansions of binary mixtures of pyrrolidine (calculated from the excess volumes reported in ref 5), *N*-methylpyrrolidine (this experiment), piperidine,[2] and *N*-methylpiperidine[1] with water at T = 298.15 K.

induced phase splitting was reported for binary aqueous solutions of 2-, 3-, and 4-methylpyridine.[75]

The excess molar expansion of *N*-methylpyrrolidine-rich mixtures ($x_1 > 0.6$) is approximately equal to zero at T = 298.15 K. At the same concentration range, E_p^E of pyrrolidine−water system is negative (Figure 11). Similar difference in the E_p^E values was observed for the mixtures of *N*-methylpiperidine[1] and piperidine,[2] although E_p^E was positive for these two systems. Thus, the contribution of methyl group to the excess molar expansion is positive: $E_p^E(CH_3) > 0$, and $(\partial S^E(CH_3)/\partial p)_T < 0$ (eq 32). Unfortunately, we cannot suggest a reliable explanation of this fact at the present stage of our studies.

Hydrogen-bonded structures affect the isentropic compressibility (κ_S) of the studied aqueous solutions in a manner typical of aqueous solutions of amines. The $\kappa_S(x_1)$ isotherms plotted in Figure 6 cross each other in narrow range of concentrations, similarly as those of binary solutions of pyridine and its methyl derivatives in water.[76−80] Thus, the compressibility is approximately independent of temperature for the mixtures within this concentration range: $\kappa_S(T) \approx$ const. This phenomenon could be explained in terms of temperature effects on instantaneous and structural compressibilities of a liquid. Studies of ultrasonic relaxation in pure water led to the conclusion that compressibility is determined by two factors: (i) instantaneous compressibility, κ_∞, due to change of intermolecular distances and to intrinsic compressibility of molecules, characterized by very short relaxation times, and (ii) structural compressibility, κ_{str}, due to disruption of hydrogen-bonded dynamic structures of water,[81] with much longer relaxation time of the picoseconds order of magnitude:[82]

$$\kappa = \kappa_\infty + \kappa_{str} \tag{36}$$

Although originally suggested for water, eq 36 was also applied to explain the temperature-independent compressibility of dilute binary aqueous solutions of nonelectrolytes in terms of clathrate-like structures in liquids.[83,84] Further studies evidenced that this independence, i.e., the $\kappa_S(T)$ = const. relationship, for the mixtures with the cavities in the framework of water filled up by the solute molecules is an approximate one, and the $\kappa_S(T)$ functions are rather slightly convex downward in the vicinity of minimum.[76,77,79] That results from counteracting effects of temperature on the instantaneous and structural contributions in compressibility. The contribution due to instantaneous compressibility increases with increasing temperature because of increased intermolecular distances, while that of the structural one decreases due to disintegration of the hydrogen-bonded structures. Thus, the compressibility of "predominantly structured" solutions de-

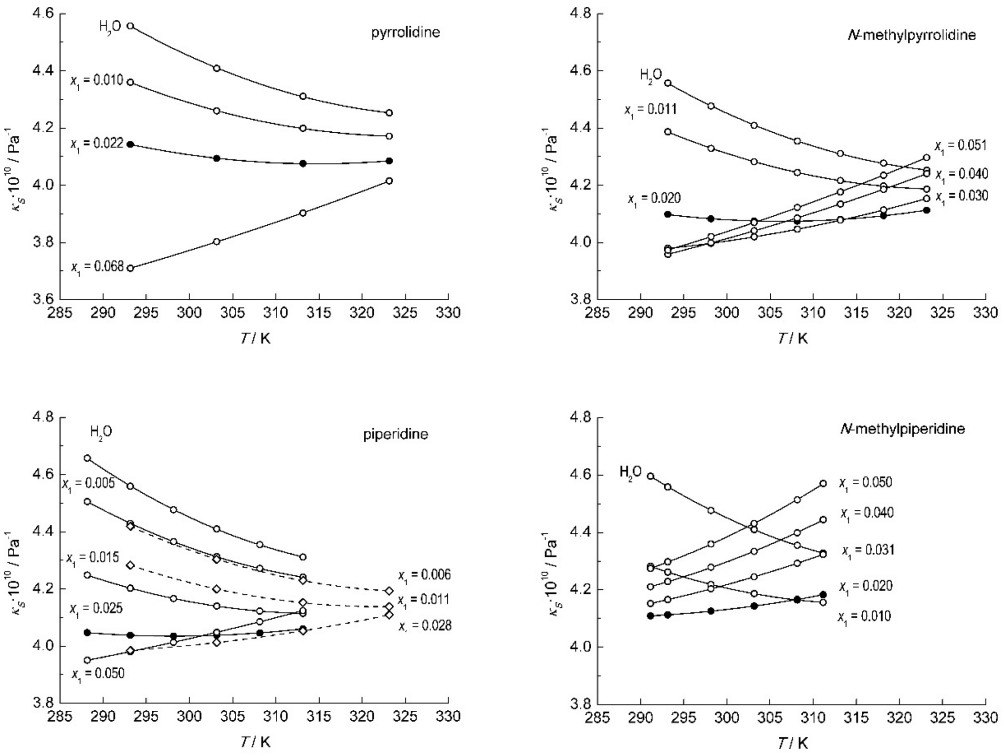

Figure 12. Isentropic compressibility of aqueous solutions of pyrrolidine,[6] piperidine (circles, ref 2; diamonds, ref 6), *N*-methylpyrrolidine (this work), and *N*-methylpiperidine.[1] Points, experimental results; lines, fitted empirical parabolas. Nearly flat functions are marked with filled symbols.

DOI: 10.1021/acs.jpcb.6b10262
J. Phys. Chem. B 2017, 121, 3070−3086

creases with temperature. If the two effects cancel each other out, compressibility becomes independent of temperature; i.e., its temperature derivative is zero. It is illustrated by the flat $\kappa_S(T)$ curves for aqueous solutions of pyrrolidine, *N*-methylpyrrolidine, piperidine and *N*-methylpiperidine plotted in Figure 12. As seen in Figure 13, the (x_1, κ_S) coordinates of T

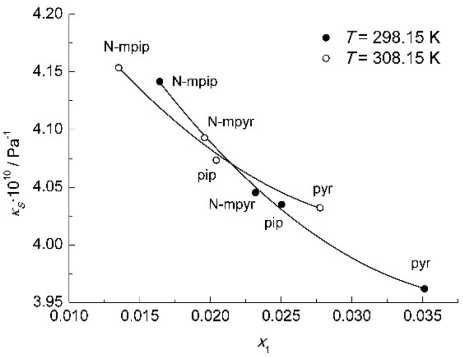

Figure 13. Interpolated coordinates of the $\kappa_S(T = \text{const}, x_1)$ minima for aqueous solutions of pyrrolidine, piperidine, *N*-methylpyrrolidine, and *N*-methylpiperidine.

= 298.15 K and T = 308.15 K isotherms minima, interpolated from the experimental results, shift toward lower amine concentrations with increasing size of the solute molecule. Indeed, the bigger the solute molecule, the larger is the number of water molecules necessary to enclose it within the hydrogen-bonded network. Consequently, the hydrogen bonds density (i.e., the number of these bonds per unit volume of the solution) is lower, and the compressibility is higher. Since at least three of the four compared amines form clathrate hydrates,[15,20] or semiclathrates[21] in the solid state, it seems reasonable to conclude that compressibility is another thermodynamic property, apart from the excess expansion, in which dynamic clathrate-like structures in dilute aqueous solutions are revealed.

It should be stressed, however, that the formation of clathrate-like hydration polyhedra around nonpolar moieties of the solute molecules suggested in this work is not a general rule for dilute aqueous solutions. On the contrary, an arrangement of water molecules in hydrogen-bonded network depends strongly on size and shape of the solute molecules, as well as on the charge distribution. For example, electrostatic repulsion predominates for tetraalkylammonium cations with short hydrocarbon chains that leads to monomolecular dispersion in aqueous solutions, while hydrophobic aggregation occurs for those with longer chains.[85] Attempts have been undertaken to correlate the size of hydrophobic parts of molecules belonging to the same class of chemical compounds with the enthalpies of solution. Heat effects of solution of tetraalkylammonium salts are correlated with the chain length for cations with short hydrocarbon chains, while rather with the volume for those with longer ones. Thus, accommodation of hydrophobic units of a moderate size creates excluded volume without disrupting water structure, since water−water hydrogen bonding simply goes around the solute. In contrast, very large hydrophobic objects appear to disrupt the H-bond network of water inducing depletion of solvent density near the apolar surface.[86,87]

6. CONCLUSIONS

The amines studied, piperidine, pyrrolidine, *N*-methylpiperidine, and *N*-methylpyrrolidine, form hydrogen-bonded complexes with water and methanol. Limiting partial molar enthalpies of solution of water and methanol in the four amines as well as the amines in methanol were assessed using a simple "chemical reaction" model, which required just binary molecular interactions energies, calculated theoretically by quantum chemical methods. The assessed values proved to be very close to the experimental enthalpies (Figure 8), although the average association numbers depended on the theoretical method by which the binary interactions energies were calculated: MP2, DFT/B3LYP, or B2PLYP. Nevertheless, the association numbers exhibited regularities independent of the theoretical method. The four amines probably form 1:1 cross-associates with methanol, independently of which one of the mixture components is the solvent, while RN·H_2O and $(RN)_2$·H_2O cross-associates occur in infinitely diluted solutions of water in the amines. The amine−water cross-association equilibrium is shifted toward $(RN)_2$·H_2O in the pyrrolidine and piperidine solvents. Methyl group at the nitrogen atom of the ring constitutes a steric hindrance that makes formation of hemihydrates less favorable because of restricted rotation of the amine molecules around the O−H···N bonds. Another reason is slightly lower association energies of the complexes of water with methyl-substituted amines (Table 1). In spite of the lower energies, the volume contraction on mixing with water is bigger for *N*-methylpyrrolidine and *N*-methylpiperidine than for their nonsubstituted counterparts (Figure 10). That is most probably because the N−H···N bonds in neat pyrrolidine and piperidine break on the formation of O−H···N bonded cross-associates with water. Different shapes of secondary and tertiary amine molecules may also affect the excess volumes, while the differences in size are probably less important, as the excess does not depend on the number of methylene groups in the amine ring.

The "chemical reaction" model involving binary molecular interactions is too simple to account for highly exothermic effects of dissolution of the amines in water. Thus, empirical contribution due to hydrophobic hydration was considered in the estimations of the limiting partial molar enthalpies of solution, along with the binary molecular interactions energies calculated by quantum chemical methods. In this manner, very good agreement of the assessed enthalpies with the calorimetric results was achieved.

The hydrophobic hydration probably consist in the formation of dynamic structures resembling those of solid semiclathrate hydrates in dilute aqueous solutions of amines. Thus, the solvent-separated arrangement of the solute molecules predominates at very low concentrations. With increasing amine concentration, the structures gradually decay and the systems become heterogeneous in the nanometer-order length scale, as results from the SANS experiments. This aggregation probably involves hydrogen bonding between hydration water molecules (Figure 9). Depending on the concentration, either just concentration fluctuations occur in such solutions, or microphase separated systems with two characteristic lengths arise. The propensity to microseparation is negatively correlated with the size of the solute molecules and it increases in the following order: *N*-methylpiperidine < *N*-methylpyrrolidine < piperidine < pyrrolidine.

DOI: 10.1021/acs.jpcb.6b10262
J. Phys. Chem. B 2017, 121, 3070−3086

■ ASSOCIATED CONTENT

Supporting Information

The Supporting Information is available free of charge on the ACS Publications website at DOI: 10.1021/acs.jpcb.6b10262.

Selected bond lengths and valence angles for the complexes optimized at the DFT/B3LYP, B2PLYP, and MP2 levels of theory; experimental enthalpies of solution, densities, excesses of molar volume, and thermal expansion; and enthalpies and volumes used in calculations by Solomonov's method (PDF)

■ AUTHOR INFORMATION

Corresponding Author

*(W.M.) E-mail: w.marczak@imp.sosnowiec.pl.

ORCID

Wojciech Marczak: 0000-0002-7323-8293

Notes

The authors declare no competing financial interest.

■ ACKNOWLEDGMENTS

This work has been supported by the European Commission under the seventh Framework Program through the Key Action: Integrated Infrastructure Initiative for Neutron Scattering and Muon Spectroscopy, NMI3-II/FP7, Contract No. 283883, Project BRR_409 "Molecular aggregates in aqueous solutions of pyrrolidine and *N*-methylpyrrolidine", by the Russian Government Program of Competitive Growth of Kazan Federal University, and by a mobility grant in the framework of the Poland–Hungary Interacademy Exchange Program. The Gaussian 09 calculations were carried out in the Wroclaw Centre for Networking and Supercomputing, WCSS, Wroclaw, Poland, under calculational Grant No. 18, and additionally in the Academic Computer Centre CYFRONET at the University of Science and Technology in Cracow, ACC CYFRONET AGH, Kraków, Poland, under Grants MNiSW/SGI3700/USlaski/111/2007 and MNiSW/IBM_BC_HS21/USlaski/111/2007.

■ REFERENCES

(1) Marczak, W.; Łężniak, M.; Zorębski, M.; Lodowski, P.; Przybyła, A.; Truszkowska, D.; Almásy, L. Water-Induced Aggregation and Hydrophobic Hydration in Aqueous Solutions of *N*-Methylpiperidine. *RSC Adv.* **2013**, *3*, 22053–22064.

(2) Marczak, W.; Hołaj-Krzak, J. T.; Lodowski, P.; Almásy, L.; Fadda, G. C. Hydrogen-Bonded Aggregates in the Mixtures of Piperidine with Water: Thermodynamic, SANS and Theoretical Studies. *Chem. Phys. Lett.* **2015**, *619*, 77–83.

(3) Cabani, S.; Conti, G.; Lepori, L. Thermodynamic Study on Aqueous Dilute Solutions of Organic Compounds. Part 1.-Cyclic Amines. *Trans. Faraday Soc.* **1971**, *67*, 1933–1942.

(4) Minevich, A.; Marcus, Y. Densities and Excess and Partial Molar Volumes of Aqueous Pyrrolidine at 25 and 50 °C and Aqueous Morpholine at 25 and 60 °C. *J. Chem. Eng. Data* **2003**, *48*, 208–210.

(5) Álvarez, E.; Gómez-Díaz, D.; La Rubia, D.; Navaza, J. M. Densities and Viscosities of Aqueous Solutions of Pyrrolidine and Piperidine from (20 to 50) °C. *J. Chem. Eng. Data* **2005**, *50*, 1829–1832.

(6) Gómez-Díaz, D.; Navaza, J. M. Speed of Sound and Isentropic Compressibility of Aqueous Solutions of Pyrrolidine and Piperidine. *J. Chem. Eng. Data* **2006**, *51*, 722–724.

(7) Gómez-Díaz, D.; Navaza, J. M.; Sanjurjo, B. Densities, Viscosities, Surface Tensions, and Speeds of Sound of Aqueous Solutions of Piperidine + Pyrrolidine + Water. *J. Chem. Eng. Data* **2007**, *52*, 1996–1999.

(8) Gómez-Díaz, D.; Navaza, J. M. Surface Behavior of Aqueous Solutions of Pyrrolidine and Piperidine. *J. Chem. Eng. Data* **2004**, *49*, 1406–1409.

(9) Wu, H. S.; Locke, W. E., III; Sandler, S. I. Isothermal Vapor-Liquid Equilibrium of Binary Mixtures Containing Pyrrolidine. *J. Chem. Eng. Data* **1990**, *35*, 169–172.

(10) Marcus, Y. Preferential Solvation in Mixed Solvents. Part 11. Eight Additional Completely Miscible Aqueous Co-Solvent Binary Mixtures and the Relationship Between the Volume-Corrected Preferential Solvation Parameters and the Structures of the Co-Solvents. *Phys. Chem. Chem. Phys.* **2002**, *4*, 4462–4471.

(11) Nishikawa, S.; Gouhara, R. Ultrasonic Relaxations in Aqueous Solutions of Piperidine and Pyrrolidine. *Bull. Chem. Soc. Jpn.* **1996**, *69*, 1855–1861.

(12) Bond, A. D.; Davies, J. E.; Parsons, S. Azetidine, Pyrrolidine and Hexamethyleneimine at 170 K. *Acta Crystallogr., Sect. C: Cryst. Struct. Commun.* **2008**, *64*, o543–o546.

(13) Dziubek, K. F.; Katrusiak, A. Pressure-Induced Pseudorotation in Crystalline Pyrrolidine. *Phys. Chem. Chem. Phys.* **2011**, *13*, 15428–15431.

(14) Budd, L. E.; Ibberson, R. M.; Marshall, W. G.; Parsons, S. The Effect of Temperature and Pressure on the Crystal Structure of Piperidine. *Chem. Cent. J.* **2015**, *9*, 18.

(15) Shin, W.; Park, S.; Koh, D.-Y.; Seol, J.; Ro, H.; Lee, H. Water-Soluble Structure H Clathrate Hydrate Formers. *J. Phys. Chem. C* **2011**, *115*, 18885–18889.

(16) Susilo, R.; Alavi, S.; Ripmeester, J.; Englezos, P. Tuning Methane Content in Gas Hydrates Via Thermodynamic Modeling and Molecular Dynamics Simulation. *Fluid Phase Equilib.* **2008**, *263*, 6–17.

(17) Strobel, T. A.; Koh, C. A.; Sloan, E. D. Water Cavities of sH Clathrate Hydrate Stabilized by Molecular Hydrogen. *J. Phys. Chem. B* **2008**, *112*, 1885–1887.

(18) Martin, A.; Peters, C. J. Hydrogen Storage in sH Clathrate Hydrates: Thermodynamic Model. *J. Phys. Chem. B* **2009**, *113*, 7558–7563.

(19) Udachin, K. A.; Ratcliffe, C. I.; Ripmeester, J. A. A Low Symmetry Form of Structure H Clathrate Hydrate, *Proceedings of the 6th International Conference on Gas Hydrates (ICGH 2008)*, Vancouver, British Columbia, Canada, July 6–10, 2008; https://circle.ubc.ca/handle/2429/1091, retrieved 05.07.2016.

(20) Shin, W.; Park, S.; Ro, H.; Koh, D.-Y.; Seol, J.; Lee, H. Phase Equilibrium Measurements and the Tuning Behavior of New sII Clathrate Hydrates. *J. Chem. Thermodyn.* **2012**, *44*, 20–25.

(21) Dobrzycki, L.; Taraszewska, P.; Boese, R.; Cyrański, M. K. Pyrrolidine and Its Hydrates in the Solid State. *Cryst. Growth Des.* **2015**, *15*, 4804–4812.

(22) Marczak, W.; Kiełek, K.; Czech, B.; Flakus, H.; Rogalski, M. Complexes of 2,6-Dimethylpyridine With Water in Condensed Phases and the Dynamical Co-Operative Interactions Involving Hydrogen Bonds. *Phys. Chem. Chem. Phys.* **2009**, *11*, 2668–2678.

(23) Marczak, W.; Czech, B.; Almásy, L.; Lairez, D. Molecular Clusters in Aqueous Solutions of Pyridine and its Methyl Derivatives. *Phys. Chem. Chem. Phys.* **2011**, *13*, 6260–6269.

(24) Zaitseva, K. V.; Varfolomeev, M. A.; Solomonov, B. N. Thermodynamics of Hydrogen Bonding of Weak Bases in Alcohol Solutions: Calorimetry of Solution, IR-spectroscopy and Vapor Pressure Analysis. *J. Mol. Struct.* **2012**, *1018*, 14–20.

(25) Solomonov, B. N.; Novikov, V. B.; Varfolomeev, M. A.; Mileshko, N. M. A New Method for the Extraction of Specific Interaction Enthalpy from the Enthalpy of Solvation. *J. Phys. Org. Chem.* **2005**, *18*, 49–61.

(26) Solomonov, B. N.; Novikov, V. B.; Varfolomeev, M. A.; Klimovitskii, A. E. Calorimetric Determination of Hydrogen-Bonding Enthalpy for Neat Aliphatic Alcohols. *J. Phys. Org. Chem.* **2005**, *18*, 1132–1137.

(27) Novikov, V. B.; Abaidullina, D. I.; Gainutdinova, N. Z.; Varfalomeev, M. A.; Solomonov, B. N. Calorimetric Determination of

the Enthalpy of Specific Interaction of Chloroform with a Number of Proton-Acceptor Compounds. *Russ. J. Phys. Chem.* **2006**, *80*, 1790−1794.
(28) Varfolomeev, M. A.; Rakipov, I. T.; Acree, W. E., Jr.; Brumfield, M.; Abraham, M. H. Examination of Hydrogen-Bonding Interactions Between Dissolved Solutes and Alkylbenzene Solvents Based on Abraham Model Correlations Derived From Measured Enthalpies of Solvation. *Thermochim. Acta* **2014**, *594*, 68−79.
(29) Zaitseva, K. V.; Varfolomeev, M. A.; Novikov, V. B.; Solomonov, B. N. Enthalpy of Cooperative Hydrogen Bonding in Complexes of Tertiary Amines with Aliphatic Alcohols: Calorimetric Study. *J. Chem. Thermodyn.* **2011**, *43*, 1083−1090.
(30) Zaitseva, K. V.; Varfolomeev, M. A.; Solomonov, B. N. Hydrogen Bonding of Aliphatic and Aromatic Amines in Aqueous Solution: Thermochemistry of Solvation. *Russ. J. Gen. Chem.* **2012**, *82*, 1669−1674.
(31) Møller, C.; Plesset, M. S. Note on an Approximation Treatment for Many-Electron Systems. *Phys. Rev.* **1934**, *46*, 618−622.
(32) Kendall, R. A.; Dunning, T. H.; Harrison, R. J. Electron Affinities of the First-Row Atoms Revisited. Systematic Basis Sets and Wave Functions. *J. Chem. Phys.* **1992**, *96*, 6796−6806.
(33) Dunning, T. H. Gaussian-Basis Sets for Use in Correlated Molecular Calculations. 1. The Atoms Boron through Neon and Hydrogen. *J. Chem. Phys.* **1989**, *90*, 1007−1023.
(34) Becke, A. D. Density Functional Thermochemistry III. The Role of Exact Exchange. *J. Chem. Phys.* **1993**, *98*, 5648−5652.
(35) Lee, C.; Yang, W.; Parr, R. G. Development of the Colle−Salvetti Correlation-Energy Formula into a Functional of the Electron Density. *Phys. Rev. B: Condens. Matter Mater. Phys.* **1988**, *37*, 785−789.
(36) Grimme, S. Semiempirical Hybrid Density Functional with Perturbative Second-Order Correlation. *J. Chem. Phys.* **2006**, *124*, 034108.
(37) Boys, S. F.; Bernardi, F. Calculation of Small Molecular Interactions by Differences of Separate Total Energies - Some Procedures with Reduced Errors. *Mol. Phys.* **1970**, *19*, 553−566.
(38) Simon, S.; Duran, M.; Dannenberg, J. J. How Does Basis Set Superposition Error Change the Potential Surfaces For Hydrogen Bonded Dimers? *J. Chem. Phys.* **1996**, *105*, 11024−11031.
(39) Frisch, M. J.; Trucks, G. W.; Schlegel, H. B.; Scuseria, G. E.; Robb, M. A.; Cheeseman, J. R.; Scalmani, G.; Barone, V.; Mennucci, B.; Petersson, G. A., et al. *Gaussian 09*, Revision A.02; Gaussian, Inc.: Wallingford, CT, 2009.
(40) Przybyła, A.; Kubica, P.; Bacior, Sz.; Lodowski, P.; Marczak, W. Water-Like Behavior of 1,2-Ethanediol in Binary Mixtures with Pyridine and its Methyl Derivatives: Thermodynamic Excesses and the O−H···N Bonds Energy. *Chem. Phys. Lett.* **2011**, *512*, 199−203.
(41) Varfolomeev, M. A.; Rakipov, I. T.; Solomonov, B. N.; Lodowski, P.; Marczak, W. Positive and Negative Contributions in the Solvation Enthalpy due to Specific Interactions in Binary Mixtures of C1−C4 *n*-Alkanols and Chloroform with Butan-2-one. *J. Phys. Chem. B* **2015**, *119*, 8125−8134.
(42) Przybyła, A.; Lodowski, P.; Marczak, W. Volumetric Properties of Binary Mixtures of 2,4,6-Trimethylpyridine with 1,2-Ethanediol, Methanol and Water, and the Association Energies of the O−H···N Bonded Complexes. *Int. J. Thermophys.* **2012**, *33*, 692−706.
(43) Czech, B.; Lodowski, P.; Marczak, W. Correlation of the O−H···N Bonds Energy with the Excess Compression of Binary Mixtures of Pyridine and its Methyl Derivatives with Methanol and Water. *Chem. Phys. Lett.* **2013**, *556*, 132−137.
(44) Rablen, P. R.; Lockman, J. W.; Jorgensen, W. L. Ab Initio Study of Hydrogen-Bonded Complexes of Small Organic Molecules with Water. *J. Phys. Chem. A* **1998**, *102*, 3782−3797.
(45) Pápai, I.; Jancsó, G. Hydrogen Bonding in Methyl-Substituted Pyridine-Water Complexes: A Theoretical Study. *J. Phys. Chem. A* **2000**, *104*, 2132−2137.
(46) Bende, A.; Almásy, L. Weak Intermolecular Bonding in *N,N′*-Dimethylethyleneurea Dimers and *N,N′*-Dimethylethyleneurea−Water systems: The Role of the Dispersion Effects in Intermolecular Interaction. *Chem. Phys.* **2008**, *354*, 202−210.
(47) Grabowski, S. J. What Is the Covalency of Hydrogen Bonding? *Chem. Rev.* **2011**, *111*, 2597−2625.
(48) Chandra Sekhar, M.; Venkatesulu, A.; Madhu Mohan, T.; Gowrisankar, M. Density Functional Theory, Natural Bond Orbital and Atoms in Molecule Analyses on the Hydrogen Bonding Interactions in 2-Chloroaniline-Carboxylic Acids. *Orient. J. Chem.* **2015**, *31*, 897−906.
(49) Perrin, D. D.; Armarego, W. L. F. *Purification of Laboratory Chemicals*, 2nd ed.; Pergamon Press: Oxford, U.K., 1980.
(50) Solomonov, B. N.; Varfolomeev, M. A.; Nagrimanov, R. N.; Novikov, V. B.; Zaitsau, D. H.; Verevkin, S. P. Solution Calorimetry as a Complementary Tool for the Determination of Enthalpies of Vaporization and Sublimation of Low Volatile Compounds at 298.15 K. *Thermochim. Acta* **2014**, *589*, 164−173.
(51) Hallén, D.; Nilsson, S.-O.; Rothschild, W.; Wadsö, I. Enthalpies and Heat Capacities for n-Alkan-1-ols in H_2O and D_2O. *J. Chem. Thermodyn.* **1986**, *18*, 429−442.
(52) Varfolomeev, M. A.; Zaitseva, K. V.; Rakipov, I. T.; Solomonov, B. N.; Marczak, W. Speed of Sound, Density, and Related Thermodynamic Excess Properties of Binary Mixtures of Butan-2-one with C1−C4 *n*-Alkanols and Chloroform. *J. Chem. Eng. Data* **2014**, *59*, 4118−4132.
(53) Dohnal, V.; Rehak, K. Determination of Infinite Dilution Partial Molar Excess Enthalpies and Volumes for Some Ionic Liquid Precursors in Water and Methanol Using Tandem Flow Mixing Calorimetry and Vibrating-Tube Densimetry. *J. Chem. Eng. Data* **2011**, *56*, 3047−3052.
(54) Abraham, M. H.; McGowan, J. C. The Use of Characteristic Volumes to Measure Cavity Terms in Reversed Phase Liquid Chromatography. *Chromatographia* **1987**, *23*, 243−246.
(55) Graziano, G. Solvation of a Water Molecule in Cyclohexane and Water. *Can. J. Chem.* **2001**, *79*, 105−109.
(56) Southall, N. T.; Dill, K. A. The Mechanism of Hydrophobic Solvation Depends on Solute Radius. *J. Phys. Chem. B* **2000**, *104*, 1326−1331.
(57) Solomonov, B. N.; Sedov, I. A.; Varfolomeev, M. A. A Method for Calculating the Enthalpy of Hydrophobic Effect. *Russ. J. Phys. Chem.* **2006**, *80*, 659−662.
(58) Graziano, G. Shedding Light on the Hydrophobicity Puzzle. *Pure Appl. Chem.* **2016**, *88*, 177−188.
(59) Solomonov, B. N.; Sedov, I. A. Quantitative Description of the Hydrophobic Effect: the Enthalpic Contribution. *J. Phys. Chem. B* **2006**, *110*, 9298−9303.
(60) Teubner, M.; Strey, R. Origin of the Scattering Peak in Microemulsions. *J. Chem. Phys.* **1987**, *87*, 3195−3200.
(61) D'Arrigo, G.; Giordano, R.; Teixeira, J. Small-Angle Neutron Scattering Studies of Aqueous Solutions of Short-Chain Amphiphiles. *Eur. Phys. J. E: Soft Matter Biol. Phys.* **2003**, *10*, 135−142.
(62) *Statistica*, version 12; data analysis software system; StatSoft, Inc.: 2014.
(63) Sum, A. K.; Sandler, S. I. Ab Initio Calculations of Cooperativity Effects on Clusters of Methanol, Ethanol, 1-Propanol, and Methanethiol. *J. Phys. Chem. A* **2000**, *104*, 1121−1129.
(64) Smets, J.; McCarthy, W.; Maes, G.; Adamowicz, L. Correlations Between Ab Initio and Experimental Data for Isolated 1:1 Hydrogen-Bonded Complexes of Pyridine and Imidazole Derivatives with Water. *J. Mol. Struct.* **1999**, *476*, 27−43.
(65) Rocher-Casterline, B. E.; Ch'ng, L. C.; Mollner, A. K.; Reisler, H. Communication: Determination of the Bond Dissociation Energy (D_0) of the Water Dimer, $(H_2O)_2$, by Velocity Map Imaging. *J. Chem. Phys.* **2011**, *134*, 211101−01−04.
(66) Almásy, L.; Cser, L.; Jancsó, G. SANS Study of 3-Methylpyridine − Heavy Water Mixtures. *Phys. B* **2000**, *276*−*278*, 446−447.
(67) Nishikawa, K.; Kasahara, Y.; Ichioka, T. Inhomogeneity of Mixing in Acetonitrile Aqueous Solution Studied by Small-Angle X-ray Scattering. *J. Phys. Chem. B* **2002**, *106*, 693−700.

DOI: 10.1021/acs.jpcb.6b10262
J. Phys. Chem. B 2017, 121, 3070−3086

(68) Almásy, L.; Jancsó, G.; Cser, L. Application of SANS to the Determination of Kirkwood−Buff Integrals in Liquid Mixtures. *Appl. Phys. A: Mater. Sci. Process.* **2002**, *74*, s1376−s1378.
(69) Perera, A. From Solutions to Molecular Emulsions. *Pure Appl. Chem.* **2016**, *88*, 189−206.
(70) Perera, A.; Mazighi, R.; Kezic, B. Fluctuations and Micro-Heterogeneity in Aqueous Mixtures. *J. Chem. Phys.* **2012**, *136*, 174516.
(71) Kezic, B.; Perera, A. Aqueous tert-Butanol Mixtures: A Model for Molecular-Emulsions. *J. Chem. Phys.* **2012**, *137*, 014501.
(72) Marcus, Y.; Ben-Naim, A. A Study of the Structure of Water and its Dependence on Solutes, Based on the Isotope Effects on Solvation Thermodynamics in Water. *J. Chem. Phys.* **1985**, *83*, 4744−4759.
(73) Marczak, W.; Giera, E. Excess and Partial Enthalpies for Mixtures of Methylpyridine Isomers with Light and Heavy Water at 298. 15 K. *J. Chem. Thermodyn.* **1998**, *30*, 241−251.
(74) Coulier, Y.; Ballerat-Busserolles, K.; Rodier, L.; Coxam, J.-Y. Temperatures of Liquid−Liquid Separation and Excess Molar Volumes of {*N*-Methylpiperidine−Water} and {2-Methylpiperidine−Water} Systems. *Fluid Phase Equilib.* **2010**, *296*, 206−212.
(75) Schneider, G. M. Phase Behavior of Aqueous Solutions at High Pressures, in: *Water. A Comprehensive Treatise. Vol. 2 Water in Crystalline Hydrates. Aqueous Solutions of Simple Nonelectrolytes*; Franks, F., Ed.; Plenum Press: New York, London, 1973; Chapter 6, pp 381−404.
(76) Ernst, S.; Marczak, W. Acoustic and Volumetric Investigations of the Hydration of γ-Picoline in Aqueous Solutions. *Bull. Polish Acad. Sci. Chem.* **1992**, *40*, 307−322.
(77) Ernst, S.; Marczak, W. Hydrophobic and Hydrophilic Interactions in Binary Mixtures of α-Picoline with Water. *Bull. Polish Acad. Sci. Chem.* **1995**, *43*, 259−278.
(78) Ernst, S.; Marczak, W.; Kmiotek, D. Ultrasonic Velocity, Density and Adiabatic Compressibility for 2,6-Dimethylpyridine + Water in the Temperature Range 293 - 318 K. *J. Chem. Eng. Data* **1996**, *41*, 128−132.
(79) Marczak, W.; Ernst, S. Effects of Hydrophobic and Hydrophilic Hydration on the Compressibility, Volume and Viscosity of Mixtures of Water with β-Picoline. *Bull. Polish Acad. Sci. Chem.* **1998**, *46*, 375−395.
(80) Marczak, W.; Banaś, A. The Hydrophobic and Hydrophilic Interactions in the System 2,4,6-Trimethylpyridine − Water in the Vicinity of and Above the Lower Critical Solution Temperature. *Fluid Phase Equilib.* **2001**, *186*, 151−164.
(81) Hall, L. The Origin of Ultrasonic Absorption in Water. *Phys. Rev.* **1948**, *73*, 775−8781.
(82) Davis, Ch. M.; Jarzynski, J. Liquid Water−Acoustic Properties: Absorption and Relaxation. In *Water. A Comprehensive Treatise. Vol. 1 The Physics and Physical Chemistry of Water*; Franks, F., Ed.; Plenum Press: New York − London, 1972; Chapter 12, pp 443−461.
(83) Endo, H. The Adiabatic Compressibility of Nonelectrolyte Aqueous Solutions in Relation to the Structures of Water and Solutions. *Bull. Chem. Soc. Jpn.* **1973**, *46*, 1106−1111.
(84) Jerie, K.; Baranowski, A.; Rozenfeld, B.; Ernst, S.; Jeżowska-Trzebiatowska, B.; Gliński, J. Positron Annihilation in and Compressibility of Water-Organic Mixtures. III. The System Water-Methanol. *Acta Phys. Pol.* **1984**, *A66*, 167−180.
(85) Huang, N.; Schlesinger, D.; Nordlund, D.; Huang, C.; Tyliszczak, T.; Weiss, T. M.; Acremann, Y.; Pettersson, L. G. M.; Nilsson, A. Microscopic Probing of the Size Dependence in Hydrophobic Solvation. *J. Chem. Phys.* **2012**, *136*, 074507−1−7.
(86) Kustov, A. V.; Korolev, V. P. Temperature and Length Scale Dependence of Tetraalkylammonium Ion − Amide Interaction. *J. Phys. Chem. B* **2008**, *112*, 2040−2044.
(87) Kustov, A. V.; Smirnova, N. L. Temperature and Length Scale Dependence of Tetraalkylammonium Ion Solvation in Water, Formamide, and Ethylene Glycol. *J. Phys. Chem. B* **2011**, *115*, 14551−14555.

DOI: 10.1021/acs.jpcb.6b10262
J. Phys. Chem. B 2017, 121, 3070−3086